CHARACTERISTICS OF MESOSCALE PRECIPITATION AREAS

by

ROBERT ALVIN HOUZE, JR.

B. S. Texas A & M University
(1967)

SUBMITTED IN PARTIAL FULFILLMENT

OF THE REQUIREMENTS FOR THE

DEGREE OF MASTER OF

SCIENCE

at the

MASSACHUSETTS INSTITUTE OF

TECHNOLOGY

January, 1969

Signature of Author.....
Department of Meteorology, January 20, 1969

Certified by.....
Thesis Supervisor

Accepted by.....
Chairman, Departmental Committee
on Graduate Students

CHARACTERISTICS OF MESOSCALE PRECIPITATION AREAS

by

ROBERT ALVIN HOUZE, JR.

Submitted to the Department of Meteorology on 20 January 1969
in Partial Fulfillment of the Requirements for
the Degree of Master of Science.

ABSTRACT

Quantitative radar and rain-gauge data taken during eight New England rain storms were studied along with conventional meteorological data to determine the characteristics of mesoscale precipitation areas and their relation to larger- and smaller-scale phenomena. Two sizes of mesoscale areas occurred in these storms; large mesoscale areas (LMSA's) were primarily 900-1,800 mi^2 in area; and small mesoscale areas (SMSA's) were mostly 100-150 mi^2 in area. In each cyclonic storm several LMSA's were found within a synoptic-scale precipitation area on the order of 10^4 mi^2 or more. Three to six SMSA's were located within each LMSA. Anywhere from 1 to 24 convective cells, each about 3 mi^2 in area, were located within the SMSA's. In thunderstorm situations the synoptic-scale precipitation area was absent, but LMSA's and SMSA's were observed. In all storms, within a precipitation area of a given scale, areas of each of the smaller scales were present. Cells lasted 0.1 to 0.5 hr, SMSA's 0.5 to 3.0 hr, LMSA's 2 to 5 hr, and synoptic-scale areas longer than 10 hr. In a given storm the precipitation falling in the cells was 2 to 10 times as intense as that falling in the surrounding SMSA's, that in the SMSA's was about twice as intense as that falling in the LMSA's, and that in the LMSA's was about twice as intense as that in the synoptic-scale areas. In a LMSA the precipitation in the cells, the SMSA's, and the area outside of the SMSA's all contributed significantly to the total deposit of water; however, the contribution from the cells was the smallest. The vertical extent of the layer of lighter precipitation in the mesoscale areas ranged from 14,000 to 35,000 ft. Convective cells located within this precipitation had depths ranging from 3,000 to 50,000 ft. The shallower ones were located in layers aloft and were completely surrounded by the lighter precipitation, while the larger ones extended from near the ground to heights above the top of the layer of lighter precipitation. For cells, each 5,000 ft of depth

corresponded roughly to 8 mm hr^{-1} in intensity and 4 min in duration. The average cell velocities were in approximate agreement ($\pm$ 25 degrees in direction; $\pm$ 50% in speed) with the winds at their steering levels (mid-cell heights) thus suggesting that advection was the dominant process influencing their motions. SMSA's moved with approximately the same velocities as the cells they contained. Irregularly-shaped LMSA's moved with approximately the same velocities as the SMSA's and cells that they contained, while band-shaped LMSA's appeared to move in a direction different from the velocities of the SMSA's and cells that they contained.

Thesis Supervisor: Pauline M. Austin
Title: Senior Research Associate

Acknowledgements

The encouragement and suggestions of Dr. Pauline M. Austin were invaluable in guiding the author through this research.

Appreciation is also expressed to Professor James M. Austin for his critical comments and to Mrs. Robert A. Houze, Jr., for typing the manuscript.

Table of Contents

		Page
List of Tables		v
List of Figures		vi
I.	Introduction	1
II.	Data and Methods of Analysis	3
	A. Data	3
	B. Methods of Analysis	5
III.	Descriptions of Individual Storms	12
	A. 29 August 1962	12
	B. 8 July 1963 (pre-frontal phase)	16
	C. 18 May 1963	18
	D. 6 December 1962	20
	E. 17 September 1963	21
	F. 12 January 1963	23
	G. 2 February 1963	24
	H. 8 July 1963 (frontal phase)	25
	I. 9 June 1965	26
IV.	Discussion of Results	27
	A. Occurrence of Precipitation Areas of Various Scales	27
	B. Shapes and Sizes	29
	C. Intensities	30
	D. Durations	31
	E. Motions	32
	F. Instrumental Bias and Subjectivity of the Analysis	33
V.	Conclusions and Suggestions for Further Study	35
	A. Conclusions	35
	B. Suggestions for Further Study	37
References		39
Tables		40
Figures		56

List of Tables

		Page
Table I.	Average number and density of small mesoscale areas and cells in each large mesoscale area.	40
Table II.	Average number and density of cells in each small mesoscale area.	41
Table III.	Average areas of large mesoscale areas.	42
Table IV.	Vertical extent of precipitation falling in large and small mesoscale areas.	42
Table V.	Average areas of small mesoscale areas.	43
Table VI.	Rainfall rates for synoptic-scale precipitation areas, large mesoscale areas, small mesoscale areas, and cells.	44
Table VII.	Rate at which water was deposited by various parts of the large mesoscale areas.	45
Table VIII.	Rate at which water was deposited by various parts of the small mesoscale areas.	46
Table IX.	Durations of large mesoscale areas, small mesoscale areas, and cells.	47
Table X.	Motions of synoptic systems, large mesoscale areas, small mesoscale areas, and cells. Winds at steering levels.	48

List of Figures

		Page
Figure 1.	Example of computer produced hourly precipitation map.	56
Figure 2.	Example of map showing PPI sequence.	57
Figure 3.	Total precipitation deposited during each hour within a 1.5×10^4 mi^2 area surrounding Cambridge, Mass., on 28-29 August 1962.	58
Figure 4.	Surface synoptic map for 0100 EST, 29 August 1962.	59
Figure 5.	Precipitation pattern for 0440 EST, 29 August 1962.	60
Figure 6.	RHI patterns for 29 August 1962.	61
Figure 7.	Rawinsonde data for Nantucket, Mass., 29 August 1962, 0700 EST.	62
Figure 8.	Rawinsonde data for Albany, New York, 29 August 1962, 0700 EST.	63
Figure 9.	Precipitation pattern for 0635 EST, 8 July 1963.	64
Figure 10.	Detailed rain-gauge trace from West Concord, Mass., 18 May 1963.	65
Figure 11.	Detailed rain-gauge trace from West Concord, Mass., 6 December 1962.	66
Figure 12.	RHI pattern for 1443 EST, 12 January 1963.	67
Figure 13.	Typical PPI pattern for 2 February 1963 as seen at intensity levels two and four.	68
Figure 14.	RHI pattern for 1538 EST, 8 July 1963.	69
Figure 15.	Schematic representation of the precipitation patterns observed in each storm.	70
Figure 16.	Histogram showing the number of small mesoscale areas observed versus their average areas.	72
Figure 17.	Diagram showing for each storm the layer containing the cells and the layer of lighter precipitation surrounding the cells.	73
Figure 18.	Cell intensity versus cell depth for all the storms.	74

Figure 19. Histograms showing the number of cells observed versus their durations for each storm. 75

Figure 20. Cell depth versus cell duration for all the storms. 76

Figure 21. Cell intensity versus cell duration for all the storms. 77

I. Introduction

Radar observations have shown that there are three scales of importance in typical precipitation patterns. In an analysis of New England storms, Austin (1968) has suggested the following definitions of the three scales.

(1) "Synoptic-scale areas" are on the order of 10^4 - 10^5 mi^2 in area and require on the order of 10 hr to pass over a point. These areas are usually found in regions of upglide motion in cyclones. Vertical velocities in these regions are on the order of 1-10 cm sec^{-1}.

(2) "Cells" are on the order of 1-10 mi^2 in area and require on the order of 1 min to pass over a point. They occur in regions of convective overturning in unstable air. Vertical velocities in these areas are on the order of 1-10 m sec^{-1}.

(3) "Mesoscale areas" are on the order of 10^2-10^3 mi^2 in area and require on the order of 1 hr to pass over a point. They are usually detected as areas having a higher radar reflectivity than their surroundings and within which cells of still higher reflectivity are found. In cyclonic storms, mesoscale areas consist of groupings of weak convective cells surrounded by stratiform precipitation. In thunderstorm situations a number of intense convective cores are surrounded by lighter precipitation in a mesoscale region. The type and magnitude of lifting which takes place within mesoscale areas, particularly outside of the cells, does not appear to be known.

The existence of these mesoscale areas motivates one to inquire into the processes which produce them and to consider their importance in the dynamics and energetics of the larger-scale circulations of the atmosphere. The significance of cellular convection to the dynamics of an extratropical cyclone was examined by Tracton (1968) who based his

computations on a simple cell model and observed rainfall amounts. He found that the release of latent heat and the vertical transport of mass and momentum accomplished by the cells were comparable in magnitude with those due to the synoptic-scale lifting. Similar computations could be made to assess the significance of the mesoscale precipitation areas if a meaningful theoretical model could be devised to compute the lifting which occurs within them.

Before an attempt is made to formulate a physical model simulating the lifting processes which produce mesoscale precipitation areas, it is necessary to obtain a set of detailed observations of their characteristics and behavior in a variety of situations. Therefore, the objective of this study is to bring together such a set of observations. This goal is accomplished by examining radar and rain-gauge data for eight New England storms which are of a wide variety of synoptic and seasonal types. From these data, the size, shape, motions, durations, and rainfall rates are determined for the mesoscale precipitation areas in each storm. The characteristics of the synoptic-scale and cellular-scale precipitation areas are also examined for each storm to determine their relationships to the mesoscale areas.

II. Data and Methods of Analysis

A. Data

1. Radar Observations. The radar data were selected from records obtained during 1962 and 1963 with the SCR-615-B and AN/CPS-9 radars located at the Massachusetts Institute of Technology. The AN/CPS-9 has a wave length of 3 cm and a beam width between half-power points of one degree. The SCR-615-B has a wave length of 10 cm and a beam width of 3 degrees. The SCR-615-B at its longer wavelength is used primarily in situations where intense convective cells are present. The AN/CPS-9 because of its shorter wavelength is used primarily in storms where light precipitation is falling over a large area. Both radars can resolve horizontal areas as small as 1-5 mi^2 depending on the range.

The radar data were in the form of photographs on 35 mm film of the Plan Position Indicator (PPI) and the Range Height Indicator (RHI). The PPI displays the averaged, range-normalized signal, quantized into a series of intensity levels. The radar equation relates the average signal intensity to the reflectivity per unit volume of the target, and the reflectivity is empirically related to the rainfall rate. The overall accuracy, according to Austin and Geotis (1960), is 2-3 db. Some of the data, however, were obtained during late 1962 and early 1963, a time at which the AN/CPS-9 was operating with a much lower accuracy. Each intensity level covered an interval of about 5 db (corresponding to a factor of two in equivalent rainfall rate). Each photograph of the PPI shows one intensity level, and the time required to photograph one complete sequence of intensity levels was usually 2-4 min. The RHI observations were obtained at selected azimuths with the AN/CPS-9 at successively

reduced gain settings. Each photograph of the RHI showed the signal at one setting.

2. Information from rain-gauge network. Hourly precipitation amounts from within 120 mi of the radar site are available for 69 stations of the U.S. Weather Bureau cooperative-observer network. The Weather Radar Research Project of the Massachusetts Institute of Technology has prepared hourly maps showing the precipitation amounts at these stations for the New England storms of 1962 and 1963. (E.g. Figure 1) For each storm, they have also prepared histograms showing the total precipitation deposited during each hour within a 1.5×10^4 mi^2 area surrounding Cambridge, Massachusetts. (E.g. Figure 3) Maps and histograms were selected for analysis from those prepared for the 1962-1963 storms.

3. Detailed rain-gauge records. Continuous records of the tipping-bucket and Hudson Jardi flowmeter rain gauges at the Weather Radar Research Project's field station in West Concord, Massachusetts, were used. These gauges have a time resolution of a few seconds in moderate and heavy precipitation and about a minute in light rain. In addition, records were obtained from tipping-bucket gauges at Weather Bureau stations in Boston, Massachusetts, and Concord, New Hampshire. These have resolutions of about one minute.

4. Conventional meteorological observations. Conventional data from publications of the U.S. Weather Bureau were used. Rawinsonde observations for Portland, Maine, Albany, New York, and Nantucket, Massachusetts, were obtained from Northern Hemisphere Data Tabulations. Hourly weather reports were obtained from Local Climatological Summaries for the following stations: Boston, Massachusetts; Concord, New Hampshire; Worcester, Massachusetts; Providence, Rhode Island; Portland, Maine; Hartford, Connecticut; Nan-

tucket, Massachusetts and Bridgeport, Connecticut. Surface and 500-mb maps were obtained from the Daily Weather Map series.

B. Methods of Analysis

1. Selection of storms. A vast amount of data was available for most of the New England storms of 1962 and 1963. Eight storms were selected, and they are listed below by date with the synoptic type (according to the classification of Kraus, 1966) also indicated:

Date	Synoptic Type
29 August 1962	Coastal low (ex-hurricane)
8 July 1963	Cyclone moving eastward from Great Lakes region
18 May 1963	Overland low plus coastal low
6 December 1962	Cyclone approaching from southwest
17 September 1963	Wave on a stationary front
12 January 1963	Wave on a stationary front
2 February 1963	Great Lakes low
9 June 1965	Air mass (thunderstorm complex)

The last storm in the list was not one of the 1962-1963 storms, although comparable data were available. In no case was there any knowledge of the type of precipitation patterns in a storm before it was chosen. And in no case was a storm rejected because of the precipitation patterns it was found to contain. The storms were selected mostly from those which were primary precipitation producers and to represent as many different synoptic and seasonal situations as possible. They were restricted to situations for which adequate radar coverage was maintained, and situations for which detailed rain-gauge traces were available were preferred.

2. Synoptic-scale analysis. The surface and upper-air pressure and wind flow patterns from the conventional maps were observed for each storm.

The hourly maps of the rain-gauge network were examined in each storm to determine whether or not a synoptic-scale precipitation area was present. An area on the order of 10^4 mi^2 within which all of the stations reported precipitation was called a synoptic-scale precipitation area. The intensity of the precipitation in such an area was estimated from the rain-gauge maps and detailed rain-gauge traces. On the maps, the reports which did not appear to be attributable to mesoscale areas or cells indicated the general level of rainfall rate in the synoptic-scale area. Similarly, the portions of the detailed rain-gauge traces which were not associated with mesoscale areas or cells also showed the level of rainfall rate in the synoptic-scale area. The hourly weather reports from Weather Bureau stations located in the synoptic-scale area indicated the type of precipitation and whether or not is was showery or non-showery.

Maps of the precipitation pattern were drawn for various times during each of the storms. An example is Figure 5. On these maps the zero contour encloses the area in which all the rain gauges were reporting precipitation. The contours for larger precipitation rates are lines of threshold reflectivity (converted to equivalent rainfall rate) for each radar intensity level. The pertinent hourly weather reports were also plotted in the standard meteorological symbols. In Figure 5 the synoptic-scale precipitation area is considered to be the area enclosed by the zero contour.

The exact sizes, areas, motions, and durations of the synoptic-scale areas were not determined because their horizontal dimensions were greater than those of the region of study.

3. Characteristics of mesoscale areas. To simplify their examination, the photographs of each intensity-level sequence on the PPI, were traced onto a single map. The tracing was done by projecting the photographs with a Richardson viewer and copying the images directly off the screen. Each map consisted of a series of contours of rainfall rate, each contour corresponding to one of the intensity levels (e.g. Figure 2).

Mesoscale areas were identified by measuring the sizes of precipitation areas which appeared in the PPI patterns. Any area larger than a cell, but smaller than a synoptic-scale area, was called a mesoscale area. It soon became apparent that some of the precipitation patterns contained two sizes of mesoscale areas: large mesoscale areas (LMSA's), 500 - 5,000 mi^2 in area; and small mesoscale areas (SMSA's), 25-500 mi^2 in area. Usually several SMSA's were located within a LMSA.

In each storm, representative mesoscale areas were selected for detailed study and their characteristics were tabulated. From the PPI maps, the sizes and shapes were determined. The average size was computed for each mesoscale area from a number of individual observations during its lifetime. The SMSA's and cells located within each LMSA and the cells located within each SMSA were counted and the numbers averaged. The average number of cells per square mile and SMSA's per square mile were computed for each LMSA. The average number of cells per square mile was also computed for each SMSA. The motions and durations of the mesoscale areas were determined by tracking them from one PPI sequence to the next.

The precipitation intensity in the mesoscale areas was estimated from the rain gauges over which the areas passed and from their radar reflectivity $Z(mm^6\ m^{-3})$ which is empirically related to the rainfall rate $R(mm\ hr^{-1})$ by

the equation $Z=200\,R^{1.6}$. For a LMSA, the precipitation intensity was estimated for the area outside of the SMSA's and cells. For a SMSA, the intensity was determined for the area outside of the cells. These rainfall rates, the average areas, the densities of cells and SMSA's, and an estimated cell area were used to compute for each LMSA, the relative amounts of water deposited per unit time by the cells, by the SMSA's outside of the cells, and by the LMSA outside of the SMSA's and cells. Similarly, for each SMSA the relative amounts deposited by the cells and by the SMSA outside of the cells were computed.

4. Characteristics of cells. Cells were identified on the PPI maps as precipitation areas 1-25 mi^2 in area. The exact horizontal sizes and shapes of cells were not determined because their dimensions were close to the limit of the horizontal resolution of the radars. Therefore, the estimated cell area of 3 mi^2 was used in the computations of water deposited by the cells. The cell motions and durations were determined by tracking them from one PPI sequence to the next. The PPI maps and the records of rain gauges over which cells passed were used to estimate the rainfall rate in a typical cell for each storm.

The precipitation in the cells which appear in the PPI patterns falls from convective elements which may be identified in the RHI photographs. The echoes at all of the gain settings for each RHI sequence were plotted on the same chart (e.g. Figure 6). The convective elements appeared as columns of precipitation with horizontal dimensions of 1-5 mi. The heights of the bottoms and tops of these convective elements were estimated from the RHI charts and the radiosonde data. The tops of the cells were assumed to coincide with the tops of the precipitation columns appearing in the RHI patterns, although lack of detectability may have caused these heights to be slightly underestimated.

The bases of cells were more difficult to locate. The echoes on the RHI show only the precipitation falling from the convective elements and therefore give no direct indication of the bases of the convective elements generating the precipitation. However, the following criteria were used to help locate cell bases. If the precipitation trailed off at an angle from a vertical column, then the level at which it began to trail off was assumed to be the bottom of the cell (e.g. Figure 12). If a stable layer was present in the soundings, and the precipitation in a column was falling through it, then the bottom of the cell was assumed to be at the top of the stable layer.

If a layer of lighter precipitation surrounding the cells was present, then its depth was also determined and recorded. In the RHI patterns, this layer usually was apparent only at very close ranges since the detectability of light precipitation decreases rapidly with range.

A cell which appears on the PPI maps is expected to move at the same horizontal velocity as the convective element which is producing it (Ligda, 1953). The motion of the convective element is generally thought to be governed by the mean wind in the layer where the hydrometeors are formed and grow (e.g. Byers and Braham, 1949). For each storm in this study, the wind near the middle of the layers containing cells was obtained from the rawinsonde data and is referred to as the "steering level wind". It is used as an approximation to the mean flow in the layer and is compared with the motions of the cells as determined from the PPI patterns.

5. Qualitative implications of the data. The method of investigation discussed above is a system of obtaining from the data quantities which are a measure of various aspects of the precipitation areas (size, motion, etc.).

There is additional insight to be gained regarding these areas by noting in a qualitative way the sort of patterns present in the data. In particular, the detailed rain-gauge traces, the RHI data, and the PPI patterns sometimes provide additional information which relates to the relative predominance of stratiform and cellular precipitation in the mesoscale areas but which cannot be tabulated in terms of specific numbers.

When a cellular mesoscale area passes over a rain gauge, the detailed record of rainfall rate shows a series of sudden rises and falls, each lasting on the order of 1 min (e.g. Figure 11). When a stratiform mesoscale area passes over a rain gauge, the trace is rather flat showing only one increase and decrease in rainfall rate during a period of the order of 1 hr (e.g. Figure 10). Many traces show these two effects in combination with sudden rises and falls occurring within periods of generally increased precipitation, thus suggesting that cells were embedded within regions of enhanced stratiform precipitation. These traces were judged subjectively to be either primarily stratiform or primarily cellular.

Additional information on the relative cellular and stratiform structure of mesoscale areas was also gained from the RHI patterns. In contrast to the columnar-appearing cells, stratiform precipitation appears to be uniform over a horizontal distance which is larger than its vertical dimension, and often a bright band, indicating the melting layer, is present. In many cases, a mixture of cellular and stratiform patterns is present. Therefore, for each storm, the RHI patterns were also examined and judged as to whether they indicated the precipitation to be primarily cellular or stratiform.

Sometimes the PPI display has a granular appearance which suggests many cells, but the cells are not defined

well enough to be counted (e.g. Figure 13a).

6. Synthesized descriptions of mesoscale areas. Each piece of information obtained both quantitatively and qualitatively as outlined above describes, for a particular storm, some aspect of the mesoscale areas or the larger- or smaller-scale phenomena to which they are related. This information was summarized for each storm by using it to form a synthesized description of the mesoscale areas occurring in that storm. The descriptions that were formed are general in that they describe the typical or average mesoscale areas in a storm, but precise in that they specify dimensions, motions, rainfall rates, etc., based on the data.

III. Descriptions of Individual Storms

A. 29 August 1962

1. Synoptic-scale pattern. This storm occurred when a tropical cyclone moved up the east coast of the United States and brought precipitation into New England. Rain fell continuously for two days in the region under observation. The histogram of the total hourly precipitation amounts for the 1.5×10^4 mi^2 area surrounding Cambridge, Massachusetts, shows that the maximum amount of rain fell between 0300 and 0400 EST (Figure 3). The period 0330-0730 EST, during and immediately following this maximum, was examined. During this time, the center of the cyclone was 55 mi east-southeast of Nantucket (Figure 4).

In Figure 5 the PPI pattern for 0440 EST is superimposed on the area contained by the zero contour which encloses all the rain-gauge stations that reported precipitation between 0400 and 0500 EST. From Figure 5 it is observed that during this hour all of the stations, except a few in the extreme northwestern and western parts of the area, were reporting precipitation. This indicates that a synoptic-scale precipitation area was present. The hourly weather reports for 0500 EST at Boston, Concord, Worcester, and Providence, also plotted in Figure 5, indicate that the precipitation in the synoptic-scale area was in the form of nonshowery rain and was occurring together with fog. The intensity of the precipitation in this area, but outside of the mesoscale areas and cells, was estimated to have been $\frac{1}{2}$-2 mm hr^{-1}.

2. Characteristics of large mesoscale areas. The precipitation pattern in Figure 5 indicates that a band-shaped large mesoscale area, referred to as LMSA A, lay within the synoptic-scale precipitation area.

Several LMSA's similar to A were observed during the passage of the storm. Evidently, they were spiral bands of the type normally observed in tropical cyclones. LMSA A was selected for detailed analysis and had the following characteristics:

Duration	240 min
Motion	
Speed	Decreased from 20 to 0 mi hr^{-1}
Direction	Toward NW
Shape	Band, oriented NNE-SSW
Ave. area	10 x 150 mi^2
Ave. no. SMSA's	5
Ave. no. cells	17
Ave. density of SMSA's	.003 mi^{-2}
Ave. density of cells	.011 mi^{-2}
Rainfall rate, outside of SMSA's and cells	5 mm hr^{-1}

3. Characteristics of small mesoscale areas. In Figure 5 there are six fairly distinct small mesoscale areas present. They are labelled A1, A2, A3, A4, A5, and A6. A1 and another SMSA, A7, which appeared later were selected for detailed investigation and their characteristics are listed below:

SMSA	A1	A7
Duration (min)	63	85
Motion		
Speed (mi hr^{-1})	25	15
Direction, toward	SW	SW
Ave. area (mi^2)	300	75
Ave. no. cells	5	4
Ave. density of cells (mi^{-2})	.017	.053
Rainfall rate in a typical SMSA, outside of cells:	10 mm hr^{-1}	

4. Cells. The larger-scale precipitation areas usually contained cells. For example, in Figure 5, several

cells of 12 mm hr^{-1} can be seen in SMSA A4 while SMSA A2 contains one of 24 mm hr^{-1}. The average number of cells contained in each of the mesoscale areas is given in the preceding sections. The rainfall rate in a typical cell was estimated to have been about 15-20 mm hr^{-1}. Sixteen cells were observed to determine the characteristic cell durations and motions. They lasted 3-18 min with an average duration of 7 min. They moved west-southwestward and southwestward at 20-30 mi hr^{-1}.

The RHI patterns in Figure 6 indicate that the cells had tops at about 15,000 ft. The rawinsonde data for 0700 EST (Figures 7 and 8) indicate that the following layers had temperature lapse rates greater than or approximately equal to the moist adiabatic lapse rate:

Portland		Albany		Nantucket	
Bottom	Top	Bottom	Top	Bottom	Top
Data Questionable		1,000	13,000	4,800	Above
		13,600	18,400		23,000

(Units: feet)

The Albany sounding is in the best agreement with the RHI data as it indicates the top of the unstable layer to have been at about 13,000 ft. This sounding also indicates that the bottom of the unstable layer was near 1,000 ft; therefore, it is reasonable to believe that the cell bottoms were probably near 1,000 ft. The steering level was taken to be at 8,000 ft. The winds at this level are listed below for the soundings taken at 0700 EST (Figures 7 and 8):

Station	Portland	Albany	Nantucket
Wind at 8,000 ft			
Direction (degrees)	060	020	020
Speed (mi hr^{-1})	35	35	20

The average cell motion is in fair agreement* with the general flow pattern defined by these winds.

5. Qualitative information concerning cellular and stratiform structure. The RHI patterns in Figure 6 contain information which is of qualitative interest at ranges 35-50 mi where the radar was looking at LMSA A. The effect of attenuation at these ranges makes the interpretation difficult; however, the echoes from LMSA A give the impression that although there are some cells definitely indicated in Figure 6a, the patterns appear to represent primarily stratiform precipitation with a bright band at 8,000 ft in Figure 6b. The lighter stratiform precipitation at these ranges appears, where detectable, to surround the cells. From the echoes at closer ranges where attenuation is not as great, it appears that the lighter precipitation extends from the ground up to 16,000 ft.

6. Synthesized description of mesoscale areas. In this section, the characteristics of the precipitation patterns in this storm are summarized on the basis of the data described above.

The one large mesoscale precipitation area (LMSA A) examined was a band-shaped region, 10 x 150 mi^2 in area and oriented NNE-SSW. On the average 5 small mesoscale areas, ranging from 75 to 300 mi^2 in area, were located within LMSA A. Outside of the SMSA's it was raining at a rate of about 5 mm hr^{-1}, while within them the rainfall rate was about 10 mm hr^{-1}. LMSA A was located within a synoptic-scale area of precipitation falling at $\frac{1}{2}$ to 2 mm hr^{-1}. Several LMSA's similar to LMSA A were observed during the course of the storm. They appeared to be spiral bands of the type normally observed in tropical cyclones.

* In these discussions agreement between velocities is defined rather loosely to be $\pm$ 25 degrees in direction and $\pm$ 50% in speeds.

LMSA A contained about 3 cells per 1,000 mi^2. The cells were primarily concentrated in the SMSA's in densities of 2 to 5 per 100 mi^2. Within the cells the rainfall rate was 15 to 20 mm hr^{-1}. They were located in the vertical between 1,000 and 15,000 ft and were completely surrounded by lighter stratiform precipitation. The cells lasted 3 to 18 min compared to 1 to 1½ hr for the SMSA's and 4 hr for LMSA A. From some of the RHI observations it appeared that the lighter stratiform precipitation surrounding the cells was more predominant than the precipitation falling from cells. This observation is in agreement with the computations of the water deposited by various parts of the large mesoscale area. LMSA A deposited a total of 3.27×10^7 m^3 hr^{-1} of water. Nine percent of this came from the cells, 69% from the SMSA's outside of the cells, and 22% from the LMSA outside of the SMSA's and cells. The cells moved toward the southwest and west-southwest at about 20-30 mi hr^{-1} in general agreement with the flow at the steering level (8,000 ft). The SMSA's also moved southwestward at about 20 mi hr^{-1}. LMSA A, however, appeared to move northwestward at a speed which decreased from 20 to 0 mi hr^{-1} during the period of observation. Thus, the resultant motion of the cells and SMSA's was southward along the band.

B. 8 July 1963 (pre-frontal phase)

For the remainder of the storms only the brief synthesized descriptions of the precipitation patterns will be given.

On 8 July 1963 a rainstorm occurred in New England preceding and during the passage of an occluded front which moved east-southeastward across the region. The character and behavior of the precipitation patterns preceding the frontal passage were so different from those more directly associated with the front itself, that the storm has been

subdivided, for the purpose of discussion, into a pre-frontal phase (denoted by 8 July 1963 (PF)) and a frontal phase denoted by 8 July 1963 (F)). The frontal phase is discussed in section III H.

For the pre-frontal phase, two large mesoscale areas (B and C), four small mesoscale areas (B1, B2, C1, C2), and eleven cells were examined in detail. The large mesoscale areas were irregular, blob-shaped regions 1,200 - 1,300 mi^2 area (e.g. LMSA B, Figure 9). They contained 3 to 4 small mesoscale areas which were 125 to 200 mi^2 in area. The rainfall rate in the small mesoscale areas was about 5 mm hr^{-1} while outside of the SMSA's in the LMSA's it was about $2\frac{1}{2}$ mm hr^{-1}. The LMSA's were located within a synoptic-scale precipitation area where the rainfall rate was $\frac{1}{2}$ to 1 mm hr^{-1}.

The large mesoscale areas contained cells in varying numbers; LMSA's B and C contained 7 and 16 cells per 1,000 mi^2 respectively. These cells were mostly located within the small mesoscale areas in densities of 1 to 4 per 100 mi^2. The rainfall rate in the cells ranged from 10 to 20 mm hr^{-1} except near the front where a few cells with intensities as great as 40 mm hr^{-1} appeared. Most of the cells lasted less than 20 min with a few lasting as long as 45 min. The SMSA's lasted about $\frac{1}{2}$ hr, and the LMSA's about $1\frac{1}{2}$ hr. The cells were located in the vertical between 3,000 and 20,000 ft and were entirely surrounded by lighter stratiform precipitation which extended from the ground up to 30,000 ft. From the RHI patterns, it appeared that the stratiform precipitation was more abundant than the cellular precipitation except in mesoscale areas nearer the approaching front where the cellular precipitation was predominant. In the following table, the total volume of water deposited per unit time by the LMSA's (averaged over their lifetimes) and the respective percentages of it which came from the LMSA's outside of the SMSA's and cells (P_L), from the SMSA's outside of the cells

(P_S), and from the cells alone (P_C) are listed:

LMSA	Total (10^7 m^3 hr^{-1})	P_L %	P_S %	P_C %
B	1.04	51	44	5
C	1.57	27	48	25

In LMSA C, which was nearer the front, cells were more numerous than in LMSA B, which was farther away from the front, and as a result they accounted for a larger percentage of the total deposit.

The motions of the cells in LMSA B exhibited considerable variation; the velocities of those observed were:

NNE	42 mi hr^{-1}
NNE	30
NE	20
NE	37
NE	45
NE	48
NE	40

but the average velocity, northeastward at 37 mi hr^{-1}, is in approximate agreement with the wind flow at the steering level (10,000 ft). LMSA B moved east-northeastward at 24 mi hr^{-1} while SMSA's B1 and B2 moved northeastward at 47 mi hr^{-1} and east-northeastward at 30 mi hr^{-1} respectively. LMSA C moved northeastward at 27 mi hr^{-1} while SMSA's C1 and C2 moved northeastward at 25 and 30 mi hr^{-1} respectively. The velocities of cells, SMSA's, and LMSA's are all in agreement within the limits which have been defined for this study ($\pm$ 25 degrees; $\pm$ 50% in speed).

C. 18 May 1963

A closed cyclonic system at 500 mb moved from just

north of Minnesota at 1300 EST on 17 May 1963 to a position over Lake Superior at 1300 EST on 18 May 1963. At this time the precipitation area associated with the storm was centered over New England. The storm subsequently moved north-northeastward and weakened.

Two large mesoscale areas (D and E), six small mesoscale areas (D1, D2, D3, E1, E2, E3), and seventeen cells were studied. The large mesoscale areas were blob-shaped and ranged from 900 to 1200 mi^2 in area. The LMSA's contained 3 to 4 small mesoscale areas which were 50 to 275 mi^2 in area. The rainfall rate in the SMSA's was about 5 mm hr^{-1}. Outside of the SMSA's in the LMSA's the precipitation was falling at 2 to 3 mm hr^{-1}. The LMSA's were located within a synoptic-scale precipitation area where the rainfall rate was 1/5 to 1/2 mm hr^{-1}.

Cells were found in the large mesoscale areas in densities of 2 to 4 per 1000 mi^2. They were mostly located within the small mesoscale areas in densities of 1 to 2 per 100 mi^2. The rainfall rate in the cells was 10 to 15 mm hr^{-1}. They lasted 4 to 20 min compared to about 1½ hr for the SMSA's and 3 to 4 hr for the LMSA's. The cells were located in the vertical in a layer between 10,000 and 19,000 ft and were completely surrounded by lighter stratiform precipitation in a layer extending from the ground up to 30,000 to 35,000 ft. The lighter precipitation appeared in the RHI patterns to be more abundant than the cellular precipitation. In the following table, the total volume of water deposited per unit time by the LMSA's and the respective percentages which fell from the LMSA's outside the SMSA's and cells (P_L), from the SMSA's outside of the cells (P_S), and from the cells alone (P_C) are listed:

LMSA	Total (10^7 m^3 hr^{-1})	P_L %	P_S %	P_C %
D	1.04	52	42	6
E	0.71	33	65	2

These figures emphasize the predominance of the stratiform precipitation in the mesoscale areas. The cells moved northeastward at 30 to 40 mi hr^{-1} in agreement with the steering level flow (at 14,500 ft). The small and large mesoscale areas also moved northeastward at 30 to 40 mi hr^{-1}.

The prevalence of stratiform precipitation in the mesoscale areas is clearly illustrated by the detailed rain-gauge trace from West Concord, Massachusetts, in Figure 10. Comparison of the PPI patterns with this trace showed that each of the rises and falls in rainfall rate was associated with the passage of a small or large mesoscale area over the rain gauge. The smooth appearance of the trace suggests that these mesoscale areas were composed of entirely stratiform precipitation; however, the corresponding PPI and RHI patterns showed that a few cells were actually located in these areas. Apparently, none of these happened to pass over the gauge.

D. 6 December 1962

At about 1300 EST on 6 December 1962 an intense cyclonic circulation moved across New England from the south-southeast. A large amount of rainfall occurred ahead of the front.

Large mesoscale areas were distinguishable in the PPI patterns at times; however, it was not possible to investigate their characteristics systematically because heavy precipitation in the vicinity of the radar site caused attenuation of the AN/CPS-9 power and therefore limited the range of detection. The LMSA's were located within a synoptic-

scale precipitation area where the rainfall rate was ½ to 1 mm hr^{-1}. Small mesoscale areas were located within this region also (presumably within the LMSA's which cannot always be clearly identified). Two of these (F1 and F2), along with eleven cells, were studied in detail. The small mesoscale areas were 50 to 100 mi^2 in area. The rainfall rate within them outside of cells was 3 to 6 mm hr^{-1}. The SMSA's contained cells in densities of 4 to 5 per 100 mi^2. The rainfall rate in the cells ranged from 10 to 50 mm hr^{-1}. Cells were located in the vertical between 11,000 and 19,000 ft. Lighter stratiform precipitation in a layer extending from the ground up to 27,000 ft completely surrounded the cells. Lifetimes of the cells ranged from 2 to 13 min while the SMSA's lasted ½ to 1 hr. The cells moved north-northwestward at 50 to 70 mi hr^{-1} in approximate agreement with the winds at the steering level (14,000 ft). The SMSA's also moved north-northwestward at 50 to 70 mi hr^{-1}.

The cellular structure of the small and large mesoscale areas in this storm is illustrated by the detailed rain gauge trace for West Concord, Massachusetts, in Figure 11. The large number of sharp peaks in this curve contrast with the smooth curve in Figure 10, the trace for 18 May 1963. Between 1536 and 1556 EST a small mesoscale area passed over the gauge producing both a general rise in the level of precipitation and several sharp peaks, one of which reached 54 mm hr^{-1}. The general rise is attributed to enhanced stratiform precipitation, and the peaks to convective cells embedded in the stratiform precipitation.

E. 17 September 1963

This storm took place when a wave formed south of New England on a stationary front and then moved northeastward at 12 mi hr^{-1} passing 100 mi west of the New England coast

at 1300 EST. This was not a particularly intense storm. A synoptic-scale precipitation area could be detected only inasmuch as several Weather Bureau stations reported drizzle and fog. Very few stations reported measurable amounts of precipitation, and those reported could be attributed to two large mesoscale precipitation areas. These two LMSA's (H and I) were studied as were two SMSA's (H1 and I1) and sixteen cells.

LMSA's H and I were blob-shaped regions, 1,300 to 1,800 mi^2 in area respectively. They each contained 5 to 6 SMSA's which were 100 to 175 mi^2 in area. The rainfall rate in the SMSA's ranged from 4 to 15 mm hr^{-1}. Outside the SMSA's in the LMSA the rainfall rate was $\frac{1}{2}$ to 1 mm hr^{-1}. The LMSA's contained about 10 cells per 1,000 mi^2. The SMSA's contained 1 to 2 cells per 100 mi^2. Cells lasted 11 min on the average, the SMSA's 2 to 3 hr, and the LMSA's longer than $3\frac{1}{2}$ hr. The cells were located in the vertical in a layer between 4,500 and 13,000 ft and were completely surrounded by a layer of lighter stratiform precipitation extending from the ground up to 14,000 ft. In the following table, the total volume of water deposited by the LMSA's per unit time and the respective percentages of it which came from the LMSA's outside of the SMSA's and cells (P_L), from the SMSA's oustide of the cells (P_S), and from the cells alone are listed:

LMSA	Total (10^7 m^3 hr^{-1})	P_L %	P_S %	P_C %
H	0.28	37	42	21
I	0.34	29	55	16

The motions of the cells varied considerably; the velocities of those observed are listed below:

In SMSA H1	
W	23
WNW	36
NW	12
NW	20
NW	40

In SMSA I1	
NW	24
W	12
WSW	13
WSW	25
SW	9
SW	17
SW	26
SW	6

The steering level winds (at 9,000 ft) were light and variable but tended to be easterly at 10 to 20 mi hr^{-1} in the vicinity of H1 and I1. Thus, the average cell velocities (WNW 26 in H1 and WSW 17 in I1) were in approximate agreement with the steering level winds. It is also noted that all of the individual cell velocities had a component of motion toward the west. The velocities of the SMSA's and LMSA's were also westward at about 10 mi hr^{-1}.

F. 12 January 1963

On this day a wave formed just off the southern coast of Cape Cod on a stationary front and moved east-northeastward at 10 mi hr^{-1}. During this time a synoptic-scale precipitation area characterized by rain, freezing rain, snow, and fog moved across New England. The PPI patterns gave some indication that large mesoscale areas were present within this region; however, several complications made it difficult to clearly identify them. The radar scanned at a maximum range of 60 mi, but the effective range was less because of low-level attenuation in wet snow. The patterns were further obscured by ground clutter near the radar site. For these reasons no characteristics of large mesoscale areas were determined. Small mesoscale areas, on the other hand, were numerous and easily identifiable. Five of them (SMSA's J1, K1, L1, M1, M2) together with twelve cells were studied

in detail.

The SMSA's ranged in sizes from 25 to 150 mi^2. Within them, except for the cells, the precipitation intensity was 1 to 2 mm hr^{-1}, compared with about $\frac{1}{2}$ mm hr^{-1} in the synoptic-scale area. Cells were present within the SMSA's in densities ranging from 3 to 24 per 100 mi^2 and were located between 13,000 and 16,000 ft. The vertical structure of the cells was deduced from RHI patterns similar to those in Figure 12. It is noted that the bottoms have been taken as being at the level where the precipitation begins to trail off at an angle. Cells lasted 3 to 20 min while the SMSA's lasted $\frac{1}{2}$ to 1 hr. Cells moved northeastward at about 45 mi hr^{-1} in rough agreement with the steering level flow (at 14,500 ft). The SMSA's moved generally northeastward at 15 to 35 mi hr^{-1}.

G. 2 February 1963

At 1300 EST on 2 February 1963 an occluded front extended southwestward from Lake Ontario. A cold front was located 100 mi behind the occluded front. Both fronts moved eastward at 35 mi hr^{-1}. By 0100 EST on 3 February 1963 the occluded front had passed New England, and the cold front was just beginning to move into the area. Preceding and during the passage of these two fronts, a synoptic-scale precipitation area passed over the area of study. As in the storm of 12 January 1963, the problems of radar detection in winter storms prevented the identification and characterization of large mesoscale areas. However, two small mesoscale areas (N1 and N2) and fourteen cells were studied in detail. The SMSA's were 100 mi^2 in area. The rainfall rate within them was 2 to 3 mm hr^{-1}, compared to $\frac{1}{2}$ to 1 mm hr^{-1} in the synoptic-scale area. The SMSA's contained 2 to 6 cells per 100 mi^2; however, these numbers may have been underestimated. The general appearance of the PPI display suggests numerous small cells

(Figure 13a), but only those which showed clearly at a higher intensity level (Figure 13b) were counted. The cells were located between 15,500 and 20,000 ft and were surrounded by lighter stratiform precipitation extending from the ground up to 22,000 ft. They lasted 3 to 12 min while the SMSA's lasted longer than 1½ hr. Cells moved mostly northeastward and occasionally eastward at speeds of 40 to 60 mi hr^{-1}. This motion was in agreement with the winds at the steering level (18,000 ft). The SMSA's moved northeastward at 45 to 50 mi hr^{-1}.

H. 8 July 1963 (frontal phase)

The pre-frontal phase of this storm was considered in section III A. The precipitation which occurred during the frontal passage is discussed in this section. No synoptic-scale precipitation area was observed during this phase of the storm. The precipitation pattern consisted of a single band-shaped large mesoscale area (LMSA P) lying along the front. LMSA P was studied along with three small mesoscale areas (SMSA's P1,P2,P3) and two cells located within it.

LMSA P was about 1,000 mi^2 in area and contained 4 SMSA's and 19 cells on the average. The precipitation in P but outside of the SMSA's was only a trace (but clearly >0). The SMSA's were about 50 mi^2 in area and the precipitation intensity within them, but outside of the cells, was 10 to 25 mm hr^{-1}. The cells had tops from 30,000 to 50,000 ft high and bases near the ground. They extended 5,000 to 15,000 ft above the lighter precipitation surrounding them. The cellular structure is dramatically illustrated by the RHI pattern of Figure 14. It is especially interesting to compare these cells with the comparatively minute cells observed on 12 January 1963 (Figure 12). The precipitation intensity inside of the cells ranged from 20 to 100 mm hr^{-1}.

The typical cell durations could not be established because of freqent interruptions of the radar data. LMSA P deposited 31.2 m^3 of water per hour. Thirty-five per cent of this came from the cells, 54% from the SMSA's, and 11% from the LMSA's. The cells moved northeastward at 25 to 30 mi hr^{-1} which was in the direction indicated by the winds at the steering level (18,000 ft), but at about one-half the speed. The SMSA's also moved northeastward, but at 30 to 40 mi hr^{-1}. The frontal band (LMSA P) apparently moved southeastward at 10 mi hr^{-1}. This motion combined with the northeastward movement of the SMSA's and cells made it appear as though the SMSA's and cells were moving from SSW to NNE along the band.

I. 9 June 1965

On this day several thunderstorm complexes were observed in the New England area in the warm air 200 mi in advance of a cold front approaching from the northwest. These complexes may be considered as small mesoscale areas. The particular complex (SMSA Q1) examined occurred near 1900 EST at which time no synoptic-scale precipitation area or large mesoscale area was observed. It was about 100 mi^2 in area and the precipitation intensity within it was 5 to 20 mm hr^{-1} outside of the cells. The cells had tops at 40,000 ft and bases near the ground. They extended about 5,000 ft above the lighter precipitation surrounding them. Within them the rainfall rate was 45-90 mm hr^{-1}. The cells lasted 15 to 50 min while the complex lasted 2½ hr. They moved eastward at 14 mi hr^{-1} which is in approximate agreement with but about 10 mi hr^{-1} slower than the wind at the steering level (18,000 ft). The complex as a whole moved southeastward at 8 mi hr^{-1}.

IV Discussion of Results

A. Occurrence of Precipitation Areas of Various Scales.

The precipitation areas occurring on each scale and the prominent synoptic-map features for each storm are shown schematically in Figure 15. They are drawn in the approximate position and with the approximate sizes and shapes which were observed. The motions of the precipitation areas and synoptic-map features as well as the winds at the steering level are also shown for each storm. Precipitation areas of all four scales were clearly observed in four of the storms, Figures 15a-15d. In the storm of 17 September 1963, Figure 15e, precipitation areas of the three sub-synoptic scales were clearly observed, but only a suggestion of light precipitation was present over a synoptic-scale region. In two of the midwinter storms, Figures 15f and 15g, a synoptic-scale area, small mesoscale areas (SMSA's), and cells were clearly present; however, since the radar observations were limited to 60 mi or less, it could not be conclusively established whether or not they contained large mesoscale areas (LMSA's). The band of precipitation associated with the frontal passage on 8 July 1963 (F), Figure 15h, contained only the three sub-synoptic scales. The air mass thunderstorm complex on 9 June 1965 (Figure 15i) contained only SMSA's and cells.

Thus, in seven of the nine storms, synoptic-scale precipitation areas were observed. Within five of the seven synoptic-scale areas, large mesoscale areas of more intense precipitation were observed, and in the other two they may have been present, but the data are inconclusive. (The findings of Nason (1965) also indicate that LMSA's are usually found within synoptic-scale precipitation areas. In a number of storms where radar echoes of large areal extent ($\gtrsim 2 \times 10^4$

mi^2) were observed, he found that in 24 out of 26 cases the large echoes contained mesoscale areas ($\sim 10^3$ mi^2) of more intense precipitation.) LMSA's were observed in six of the storms, and they contained SMSA's and cells. All nine storms contained SMSA's with cells located within them. These observations suggest that within precipitation areas of one scale, more intense areas of each of the successively smaller scales will be found.

In cyclonic storms, all four scales tend to be present (Figures 15a - 15f), although the synoptic-scale areas may, at times, appear only rather weakly as drizzle, fog, or widespread cloudiness. In situations such as the frontal band in Figure 15h or the air mass thunderstorm complex in Figure 15i, synoptic-scale precipitation areas are completely lacking.

At various times during the lifetime of each LMSA, the SMSA's and cells within it were counted. The average numbers and densities are listed in Table I. These data show that the LMSA's contained roughly the same number of SMSA's in each case, but the number of cells was quite variable.

The cells within each SMSA were also counted and their average numbers and densities are listed in Table II. Both the numbers and densities vary over a wide range of values. The variability of cell densities is as great within a single storm (12 January 1963) as from one storm to another. Thus, some SMSA's were primarily stratiform while others were primarily cellular, even within the same storm.

It is recognized that the results just summarized and those discussed below are drawn from a small sample of data and require further statistical verification. They are, at least, not predetermined in any way since the storms were selected for study without previous knowledge of the precipitation patterns they contained.

B. Shapes and Sizes

1. Synoptic-scale areas. Neither the shapes nor the exact sizes of synoptic-scale areas were determined because they extended beyond the limits of the region of study.

2. Large mesoscale areas. The large mesoscale areas were classified as being either band- or blob-shaped. LMSA A (Figure 15a) was a band-shaped area associated with a tropical cyclone. LMSA P (Figure 15h) was a band-shaped region lying along an occluded front. The other LMSA's were all blob-shaped.

The average areas of each of the LMSA's analyzed are listed in Table III. Although by definition LMSA's may be 500 - 5000 mi^2 in area, the eight in the sample are in the rather narrow range from 900 to 1800 mi^2. Thus, the data suggest that LMSA's may have preferred sizes within their defined scale.

Precipitation in the mesoscale areas was assumed to extend as high as the weakest stratiform echoes which appeared in the RHI patterns. Since these echoes could be seen only at very short ranges, measurements could not be made in each specific LMSA and SMSA. Therefore, all the LMSA's and SMSA's in a storm were assumed to have the same vertical extent as estimated from a few such limited observations. These heights, listed in Table IV, can be regarded as vertical dimensions for what heretofore have been called mesoscale "areas". These dimensions varied considerably from one storm to another, as can be noted from Table IV, the values ranging from 14,000 to about 35,000 ft.

3. Small mesoscale areas. The SMSA's were generally of irregular shapes, although some tended toward having band shapes.

Average areas of the SMSA's are listed in Table V and also plotted in a histogram (Figure 16). It is observed

from Figure 16 that most of the SMSA's had areas of 50-150 mi^2.

The vertical extent of the precipitation in the SMSA's is listed in Table IV.

4. Cells. Since cells are close to the limit of the radar resolution in horizontal dimension, they appear round in shape, and their exact horizontal area cannot be determined. Most of them appeared to be about 3 mi^2 in area and this value was assumed for computational purposes.

The vertical extent of the cells and of the lighter precipitation surrounding them is indicated schematically in Figure 17. The cells ranged in depth from 3,000 ft on 12 January 1963 to 40,000 - 50,000 ft on 8 July 1963 (f) and 9 June 1965. The shallower cells were located in layers aloft and entirely surrounded by lighter precipitation, while the deepest ones tended to extend all the way down to the ground and to protrude above the lighter precipitation.

C. Intensities

The rainfall rates observed during the various storms are listed in Table VI. It is noted that the rates in Table VI were determined for the regions within:

(a) Synoptic-scale areas, but outside of the LMSA's SMSA's, and cells;

(b) Large mesoscale areas, but outside of the SMSA's and cells;

(c) ~~Cells.~~ SMSA (d) Cells

In each of the storms, the precipitation rate increased by about a factor of two from (a) to (b) and from (b) to (c). The increase was somewhat sharper from (c) to (d), as it ranged from a factor of two to a factor of ten. The fact that the intensity always increased from one scale to the next illustrates that the larger areas were not simply groupings of

the smaller ones, but contained enhanced lighter precipitation as well.

The cell intensities were related to their depths. The rainfall rate in an average cell is plotted versus the cell depth in Figure 18. Each point corresponds to one of the storms which were studied. The straight line of best least square fit indicates an increase in intensity with depth of 8 mm hr^{-1} for 5,000 ft in depth.

Tables VII and VIII show the total volume of water deposited per unit time by each LMSA and SMSA and the percentages of it which came from (b), (c), and (d), denoted by P_L, P_S, and P_C respectively. P_L, P_S, and P_C are averages taken over the duration of the LMSA or SMSA to which they refer. Each accounted for significant parts of the total in most cases; however, P_C was almost always the smallest of the three.

D. Durations

1. Large mesoscale areas. The durations of the LMSA's, SMSA's, and cells were obtained by tracking them from one PPI sequence to the next and are listed in Table IX for each storm.

The durations of the LMSA's varied by almost a factor of ten, from 75 to 720 min. The two LMSA's observed on 18 May 1963 lasted approximately the same length of time. This may indicate that the durations of the LMSA's occurring in the same storm tend to be similar, although in different storms they vary greatly.

2. Small mesoscale areas. The durations of the SMSA's (Table III) also varied by about an order of magnitude, from 20 to 195 min. Since many of the SMSA's could not be tracked for their whole lifetimes, it is difficult to categorize their durations. However, about one-half of them had durations less

than or equal to 60 min, while the rest had durations greater than 60 min. There is some evidence that the durations may not have varied as greatly within a given storm as from one storm to another. The duration tended to vary by less than a factor of three within single storms.

3. Cells. Durations of cells are on the order of a few minutes as compared to 1 hr for the SMSA's and a few hours for the LMSA's (Table III). Since cells were considerably more numerous than SMSA's or LMSA's their durations could be treated in a more statistical manner. The durations of several representative cells were measured and then plotted in histograms showing number of cells versus duration for each storm (Figure 19). In all of the storms, except 8 July 1963 (PF) and 9 June 1965, the number of cells clearly increases as the duration decreases, with very few durations exceeding 14 min. On 8 July 1963 (PF) and 9 June 1965, however, durations greater than 14 min were common. In any of the storms, cell durations greater than 26 min were extremely rare.

The durations of cells were related to their depths and intensities. The cell depth is plotted versus cell duration in Figure 20. Each point corresponds to one of the storms studied. The line of best least square fit indicates that a cell lasted 4 min for every 5,000 ft of depth. A similar plot of cell intensity versus cell duration (Figure 21), suggests that a cell lasted 4 min for each 8 mm hr^{-1} of intensity.

E. Motions

1. Cells. The motions of cells, SMSA's, LMSA's and synoptic-scale systems in each storm are listed in Table K. These data are also shown schematically in Figure 15 where the motions are represented by vectors associated with the cells, SMSA's, LMSA's, and synoptic-scale systems. In the figure the steering level winds are indicated by the usual

wind barbs. The flow patterns indicated by this representation were compared with the average cell motions. It can be seen from Figure 15 that the average cell velocities were in rough agreement (± 25 degrees in direction; ± 50% in speed) with the steering level flow. In some storms, the cell motions were quite variable (by as much as 90 degrees in direction on 17 September 1963). Thus, the agreement with the steering level flow quoted above refers to the mean cell motion for a given storm.

2. Mesoscale areas. As a small or large mesoscale area moves, its shape changes continuously; therefore, there is always some uncertainty about its motion. However, the rough determinations of this study (Table VIII, Figure 15) show that the motions of the SMSA's were approximately the same (± 25 degrees in direction; ± 50% in speed) as those of the cells they contained. One exception is noted. The thunderstorm complex of 9 June 1965 (SMSA Q) moved to the right of the cell velocities.

The blob-shaped LMSA's moved in approximately the same manner (± 25 degrees in direction; ± 50% in speed) as the cells and SMSA's which they contained (Table VIII and Figure 15). The band-shaped LMSA's (A and P in Table VIII) appeared to move perpendicular to themselves while the SMSA's and cells which they contained moved to the left of this motion so that, in effect, the SMSA's and cells were moving along the bands. The apparent movement of a band might be an effect of viewing only a segment of a band as it moves across a fixed area. In such a case the band necessarily appears to be moving perpendicular to itself. The band-shaped LMSA P apparently was moving in conjunction with an occluded front (Figure 15h).

F. Instrumental Bias and Subjectivity of the Analysis

Large and small mesoscale areas and cells were recog-

nized as separate entities which appear when the radar data are quantized into intensity levels, each with an interval of approximately 5 db in radar reflectivity or a factor of two in equivalent rainfall rate. Since in actual storms there is a continuous gradient in precipitation rate, both the indicated sizes and intensities of the precipitation areas are influenced to a certain extent by the thresholds for each level. The factor of two difference in intensity between LMSA's and synoptic-scale areas and between SMSA's and LMSA's observed in most of the storms (Section IV C) was probably related, in some degree, to the factor of two difference between radar-intensity levels. This bias may have some influence on the precision of this study, but it does not obscure the general fact that in all the storms studied there was an orderly appearance of cells within SMSA's, SMSA's within LMSA's, and LMSA's within synoptic-scale areas and that these features had definitely recognizable characteristics.

Also, two small or large mesoscale areas sometimes appeared so close to one another that it was not quite clear whether to call them a single precipitation area or two separate areas. The decision of which to call them was subjective, but the resulting uncertainty was probably only of a factor of two which has no serious effect on the conclusions of the study.

V Conclusions and Suggestions for Further Study

A. Conclusions

Precipitation patterns in eight storms were studied for the purpose of gaining information concerning the nature of mesoscale precipitation areas. Previous studies of radar data (e.g. Austin, 1968) have shown that mesoscale areas consisting of groupings of convective cells surrounded by stratiform precipitation usually appear in cyclonic storms. It is also known that thunderstorms usually occur in mesoscale areas with several intense convective cores surrounded by lighter precipitation. The eight storms which were selected for study included various cyclonic and thunderstorm situations. The mesoscale precipitation areas occurring in each were examined with regard to their characteristics and their relationships to larger- and smaller-scale phenomena. In the early stages of the analysis it became apparent that often two distinct sizes of mesoscale areas were present, with several smaller ones appearing within each larger one. This observation prompted the following definitions:

(1) Synoptic-scale precipitation areas are those of the order of 10^4 mi^2 or more in area;

(2) Large mesoscale areas (LMSA's) are from 500 to 5,000 mi^2 in area;

(3) Small mesoscale areas (SMSA's) are from 25 to 500 mi^2 in area;

(4) Cells are smaller than 25 mi^2.

The storms which were analyzed contained seven synoptic-scale precipitation areas and many of the smaller-sized ones. Eight LMSA's, 25 SMSA's, and 125 cells were selected for systematic study. It was found that the observed size range for each scale was considerably smaller than the one defined.

The observed sizes were:

Cells.....3 mi^2
SMSA's.....100-150 mi^2
LMSA's.....900-1,800 mi^2

The dimensions of the synoptic-scale areas were not determined since they were greater than the dimensions of the region of study.

Within a precipitation area of any given scale, areas of all the smaller scales were usually present. The LMSA's normally contained 3-6 SMSA's at any given time, whereas the SMSA's contained anywhere from 1 to 24 cells.

Typically the cells lasted 0.1-0.5 hr, SMSA's 0.5-3.0 hr, LMSA's 2-5 hr, and synoptic-scale areas longer than 10 hr. Thus, within an area of a given scale the pattern of smaller-sized areas was constantly changing.

Intensity of precipitation in areas of any scale varied considerably from storm to storm, but in any given storm the precipitation falling in the cells was 2-10 times as intense as that falling in the surrounding SMSA's; that in the SMSA's was about twice as intense as that falling in the surrounding LMSA's; and that in the LMSA's was about twice as intense as that falling in the synoptic-scale areas within which they were located. The majority of the total water deposited by a SMSA came from the stratiform parts of the area surrounding the cells rather than from the cells themselves, although both contributions were significant. In a LMSA the contributions from the cells, from the SMSA's outside of the cells, and from the parts of the LMSA outside of the SMSA's and cells were all significant, although that from the cells was usually the smallest.

The vertical extent of the precipitation in the mesoscale areas (both SMSA's and LMSA's) ranged from 14,000 to 35,000 ft. Convective cells located within the mesoscale

areas had depths ranging from 3,000 to 50,000 ft. The shallower ones were located in layers aloft and were completely surrounded by lighter stratiform precipitation. The deepest ones extended down to the ground and above the lighter precipitation. For cells there was a correlation between depth, duration, and intensity, with 5,000 ft in depth corresponding roughly to 8 mm hr^{-1} in intensity and 4 min in duration.

The average cell velocities were in approximate agreement with the winds at their steering levels (mid-cell heights). Thus, advection must have been the dominant process influencing the cell motions. SMSA's moved with approximately the same velocities as the cells they contained. Mesoscale areas, both large and small, were generally irregular in shape. Two of the LMSA's, however, were in the shape of well-defined bands. The irregular, blob-shaped LMSA's moved in roughly the same manner as the SMSA's and cells within them. The motions of band-shaped LMSA's differed from those of the smaller-scale areas within them. Their motions may be related to the motions of the synoptic-scale systems in which they are located, but there were too few cases to verify this possibility.

B. Suggestions for Further Study

The characteristics of mesoscale precipitation areas and their relation to larger- and smaller-scale phenomena have been described but need to be established in a more statistically significant way. Studies of larger samples of data will be feasible with the WR-66 radar now in operation at the Weather Radar Research Laboratory at M.I.T. and the digital data processor presently being constructed. The radar has high resolution and good coverage, and the digital output is suitable for time and space correlations of the precipitation patterns.

In addition to obtaining better descriptions of mesoscale phenomena future research should be directed toward determining the physical basis for the occurrence of mesoscale precipitation areas and toward the development of dynamical models describing their behavior. Such models could be used to assess the effect of the lifting process in mesoscale areas on the dynamics and energetics of the larger-scale circulations of the atmosphere.

One particular problem of interest is concerned with the reasons for which small mesoscale areas arise. Two hypotheses may be advanced to explain why the precipitation immediately surrounding the cells (i.e. the precipitation of the SMSA's) is more intense than that in the surrounding region (the LMSA). This enhancement may be due to intensified lifting in regions on the order of 100 mi^2 in area; or it may come about when cloud and precipitation particles which develop in the convective updrafts are carried out of the upper portions of cells and thereby added to the precipitation which has originated outside of the cells. This latter possibility has been shown by Melvin (1968) to be feasible in the case of thunderstorm complexes. The relationship between the cells and the SMSA's may be investigated by making calculations based on models of the air motions and the growth of precipitation particles originating inside and outside of cells. Models appropriate to both hypotheses should be considered. The results of such computations would be compared to observed data to determine which assumptions lead to more realistic precipitation patterns. The data used in this study, in addition to conventional data, should consist of improved measurements of the radar reflectivity in three dimensions (as can be obtained with the WR-66 radar), continuous sampling of the raindrop sizes at the surface (for example with the Joss raindrop spectrometer (Joss and Waldvogel, 1967)), and frequent radiosonde observations.

References

Austin, P. M., 1968: Analysis of small-scale convection in New England. Proc. Thirteenth Radar Meteorology Conf., Boston: American Meteorological Society, 210-215.

Austin, P. M., and Spiros Geotis, 1960: The radar equation parameters. Proc. Eighth Weather Radar Conf., Boston: American Meteorological Society, 15-22.

Byers, H. R., and R. R. Braham, Jr., 1949: The Thunderstorm, Washington: U. S. Weather Bureau.

Joss, J., and A. Waldvogel, 1967: Ein Spectrograph für Niederschlagstropfen mit automatischer Auswertung. Pure and Applied Geophysics, Vol. 68, 240-246.

Kraus, M. J., 1966: Areal and spatial distributions of precipitation in New England storms. B.S. Thesis, Dept. of Geology and Geophysics, M.I.T., Cambridge, Mass., 53 pp.

Ligda, Myron G. H., 1953: The horizontal motion of small precipitation areas as observed by radar. M.I.T. Weather Radar Research: Tech. Rept. No. 21, 60 pp.

Melvin, G. L., 1968: The development of thunderstorm complexes and their associated vertical transports. S.M. Thesis, Dept. of Meteorology, M.I.T., Cambridge, Mass., 65 pp.

Nason, C. K., 1965: Mesoscale precipitation patterns in Central New England. S.M. Thesis, Dept. of Meteorology, M.I.T., Cambridge, Mass., 99 pp.

Tracton, M. S., 1968: The role of cellular convection within an extratropical cyclone. Proc. Thirteenth Radar Meteorology Conf., Boston: American Meteorological Society, 216-221.

U. S. Department of Commerce, Weather Bureau; 1962, 1963, 1965: Local Climatological Data.

U. S. Department of Commerce, Weather Bureau; 1962, 1963, 1965: Daily Series, Synoptic Weather Maps, Part II, Northern Hemisphere Data Tabulations, Daily Bulletins.

U. S. Department of Commerce, Weather Bureau; 1962, 1963, 1965: Daily Weather Map.

Table I. The average number of small mesoscale areas (N_S) and cells (N_C) in each large mesoscale area (LMSA) and the average density of small mesoscale areas (D_S) and cells (D_C) in each LMSA.

Date	LMSA	N_S	D_S (10^{-3} mi^{-2})	N_C	D_C (10^{-3} mi^{-2})
29 Aug 62	A	5	3	17	11
8 Jul 63 (PF)	B	3	2	8	7
	C	4	3	21	16
18 May 63	D	3	2	8	7
	E	4	4	3	3
17 Sep 63	H	5	4	14	11
	I	6	3	16	9
8 Jul 63 (F)	P	5	5	19	19

Table II. The average number of cells (n_c) and the average density of cells (d_c) in each small mesoscale area (SMSA).

Date	SMSA	n'_c	d'_c (10^{-2} mi^{-2})
29 Aug 62	A1	5	2
	A7	4	5
8 Jul 63 (PF)	B1	5	1
	B2	4	2
	C1	3	2
	C2	7	4
18 May 63	D1	1	1
	D2	1	1
	D3	1	2
	E1	2	1
	E2	1	1
	E3	1	2
6 Dec 62	F1	2	4
	G1	5	5
17 Sep 63	H1	2	2
	I1	1	1
12 Jan 63	K1	5	3
	L1	6	8
	M1	4	8
	M2	6	24
2 Feb 63	N1	6	6
	N2	2	2
8 Jul 63 (F)	P1	5	10
9 Jun 65	Q1	3	3

Table III. Average areas of large mesoscale areas (LMSA's).

Date	LMSA	Area (mi^2)
29 Aug 62	A	1500
8 Jul 63 (PF)	B	1200
	C	1300
18 May 63	D	1200
	E	900
17 Sep 63	H	1300
	I	1800
8 Jul 63 (F)	P	1000

Table IV. Vertical extent of precipitation falling in large and small mesoscale areas.

Date	Height
29 Aug 62	16,000 ft
8 Jul 63 (PF)	30,000
18 May 63	30,000 - 35,000
6 Dec 62	27,000
17 Sep 63	14,000
12 Jan 63	16,000
2 Feb 63	22,000
8 Jul 63 (F)	≅35,000
9 Jun 65	≅35,000

Table V. Average areas of small mesoscale areas (SMSA's).

Date	SMSA	Area (mi^2)
29 Aug 62	A1	300
	A7	75
8 Jul 63 (PF)	B1	125
	B2	125
	C1	125
	C2	200
18 May 63	D1	175
	D2	125
	D3	50
	E1	275
	E2	75
	E3	50
6 Dec 62	F1	50
	G1	100
17 Sep 63	H1	100
	I1	175
12 Jan 63	J1	100
	K1	150
	L1	75
	M1	50
	M2	25
2 Feb 63	N1	100
	N2	100
8 Jul 63 (F)	P1	50
9 Jun 65	Q1	100

Table VI. Rainfall rates in mm hr^{-1} for synoptic-scale precipitation areas (R_S), large mesoscale areas (R_{LM}), small mesoscale areas (R_{SM}), and cells (R_C) in each storm.

Date	R_S	R_{LM}	R_{SM}	R_C
29 Aug 62	½-2	5	10	15-20
8 Jul 63 (PF)	½-1	2½	5	10-20 (LMSA B)
				10-40 (LMSA C)
18 May 63	¼-½	2-3	5	10-15
6 Dec 62	½-1	*	3-6	10-50
17 Sep 63	0-Trace	½-1	2	4-15
12 Jan 63	½	*	1-2	3-4
2 Feb 63	½-1	*	2-3	5-10
8 Jul 63 (F)	0	½-5	5-25	20-100
9 Jun 65	0	0	5-20	45-90

* Not possible to determine

Table VII. Water deposited by various parts of the large mesoscale areas. P_L = average volume of water falling per unit time from a large mesoscale area (LMSA), outside of small mesoscale areas and cells. P_S = average volume of water falling per unit time from the small mesoscale areas, outside of the cells. P_C = average volume of water falling per unit time from the cells.

LMSA	Total (10^7 m^3 hr^{-1})	P_L %	P_S %	P_C %
A	32.7	22	69	9
B	10.4	51	44	5
C	15.7	27	48	25
D	10.4	52	42	6
E	7.1	33	65	2
H	2.8	37	42	21
I	3.4	29	55	16
P	31.2	11	54	35

Table VIII. Water deposited by various parts of the small mesoscale areas. P_S = average volume of water falling per unit time from a small mesoscale area (SMSA), outside of cells. P_C = average volume of water per unit time falling from the cells.

SMSA	Total (10^6 m^3 hr^{-1})	P_S %	P_C %
A1	80.5	91	9
A7	22.1	75	25
B1	16.9	93	7
B2	17.7	87	13
C1	20.8	72	28
C2	36.6	63	37
D1	23.2	96	4
D2	16.7	94	6
D3	7.0	86	14
E1	36.6	95	5
E2	10.0	95	5
E3	7.0	86	14
F1	9.7	52	48
G1	21.5	46	54
H1	6.3	77	23
I1	9.6	92	8
J1	—	—	—
K1	6.6	79	21
L1	3.8	57	43
M1	2.6	58	42
M2	1.9	14	86
N1	8.8	60	40
N2	7.2	84	16
Q1	36.7	37	63
P1	39.2	60	40

Table IX. Durations in minutes of large mesoscale areas (LMSA's), small mesoscale areas (SMSA's), and cells.

Date	LMSA	Dur	SMSA	Dur	Range of cell dur	Average cell dur
29 Aug 62	A	240	A1	65	3-18	7
			A7	85		
8 Jul 63 (PF)	B	80	B1	20	8-44	18
			B2	40		
	C	>80*	C1	25		
			C2	>30		
18 May 63	D	200	D1	20	4-20	8
			D2	>60		
			D3	>30		
	E	240	E1	55		
			E2	50		
			E3	>35		
6 Dec 62		**	F1	45	2-13	9
			G1	>35		
17 Sep 63	H	>210	H1	140	4-32	11
	I	>210	I1	>195		
12 Jan 63		***	J1	35	3-20	7
			K1	65		
			L1	35		
			M1	>29		
			M2	90		
2 Feb 63		***	N1	>95	3-12	5
			N2	>87		
8 Jul 63 (F)	P	720	P1	**	**	**
			P2	**		
			P3	**		
9 Jun 65		****	Q1	150	15-50	26

*Durations preceeded by > could not be determined more precisely because the data was interrupted.
**Duration was not determined.
***LMSA's were not clearly identified.
****LMSA's were not present.

Table X. Motions of synoptic systems, large mesoscale areas (LMSA's), small mesoscale areas (SMSA's), and cells. Winds at steering levels. Speeds are in miles per hour. Directions are those toward which precipitation areas are moving and from which winds are blowing. These data are illustrated schematically in Figure 15.

Date:	29 Aug 62
Synoptic map feature:	Tropical storm center
Motion:	NE 9
LMSA:	A
Shape:	Band (SSW-NNE)
Motion:	NW; speed decreased from 20 to 0 mi hr^{-1}
SMSA:	A1 A7
Motion:	SW 25 SW 15
Cell motion:	WSW-SW 20-30
Steering level winds:	
Portland	060/35 deg/mi hr^{-1}
Albany	020/35
Nantucket	020/20
Height of steering level	8,000 ft
Time of wind observation	0700 EST

Table X. (cont.)

Date:	8 Jul 63 (PF)
Synoptic map feature:	Occluded front
Motion:	SE 12
LMSA:	B C
Shape:	Blob Blob
Motion:	ENE 24 NE 27
SMSA:	B1 B2 C1 C2
Motion:	NE 47 ENE 30 NE 25 NE 30
Cell motion:	LMSA B: NE-NNE 20-48 Ave. NE 37 LMSA C: NE 30-40
Steering level winds:	
Portland	230/35 deg/mi hr^{-1}
Albany	250/45
Nantucket	220/20
Height of steering level	10,000 ft
Time of wind observation	0700 EST

Table X. (cont.)

Date:	18 May 63					
Synoptic map feature:	Low center					
Motion:	NNE 12					
LMSA:	D			E		
Shape:	Blob			Blob		
Motion:	NE 30			NE 30		
SMSA:	D1	D2	D3	E1	E2	E3
Motion:	NE 25	NE 35	NE 34	NE 36	NE 35	NE 30
Cell motion:	NE 30-40					
Steering level winds:						
Portland	180/25 deg.mi hr^{-1}			No report		
Albany	230/35			230/35		
Nantucket	220/25			220/30		
Height of steering level	14,500			14,500		
Time of wind observation	0700 EST			1900 EST		

Table X. (cont.)

Date:	6 Dec 62	
Synoptic map feature:	Cold front	
Motion:	NW 33	
LMSA:	Could not track	
SMSA:	F1	G1
Motion:	NNW 52	NNW 60
Cell motion:	NNW 50-70	
Steering level winds:		
Portland	No report	
Albany	130/80 deg/mi hr^{-1}	
Nantucket	170/85	
Height of steering level	14,500 ft	
Time of wind observation	1900 EST	

Table X. (cont.)

Date:	17 Sep 63	
Synoptic map feature:	Low center	
Motion:	NE 12	
LMSA:	H	I
Shape:	Blob	Blob
Motion:	Could not determine	W 7
SMSA:	H1	I1
Motion:	W 12	W 9
Cell motion:	LMSA H: W-NNW-NW 12-40 Ave. WNW 26	LMSA I: NW-W-SW 6-26 Ave. WSW 17
Steering level winds:		
Portland	080/10 deg/mi hr^{-1}	
Albany	050/20	
Nantucket	180/10	
Height of steering level	9,000 ft	
Time of wind observation	0700 EST	

Table X. (cont.)

Date:	12 Jan 63				
Synoptic map feature:	Low center				
Motion:	ENE 10				
LMSA:	Not clearly defined				
SMSA:	J1	K1	L1	M1	M2
Motion:	NE 15	NE 20	NE 35	NE 35	NE 25
Cell motion:	NE 45				
Steering level winds:					
Portland	240/55 deg/mi hr^{-1}				
Albany	250/55				
Nantucket	250/55				
Height of steering level	14,500 ft				
Time of wind observation	1900 EST				

Table X. (cont.)

Date:	2 Feb 63
Synoptic map feature:	Occluded front
Motion:	E 34
LMSA:	Not clearly defined
SMSA:	N1 N2
Motion:	NE 45 NE 50
Cell motion:	E NE 40-60
Steering level winds:	
Portland	250/45 deg/mi hr^{-1}
Albany	240/55
Nantucket	270/35
Height of steering level	18,000 ft
Time of wind observation	1900 EST

Table X. (cont.)

Date:	8 Jul 63 (F)			9 Jun 65
Synoptic map feature:	Occluded front			Cold front
Motion:	E 6			SE 10
LMSA:	P			No LMSA's
Shape:	Band (SSW-NNE)			present
Motion:	SE 10			
SMSA:	P1	P2	P3	Q1
Motion:	NE 30	NE 40	NE 40	SE 8
Cell motion:	NE 25-30			E 14
Steering level winds:				
Portland	220/60 deg/mi hr^{-1}			270/20
Albany	250/75			260/30
Nantucket	270/30			250/40
Height of steering level	18,000 ft			18,000 ft
Time of wind observation	1900 EST			1900 EST

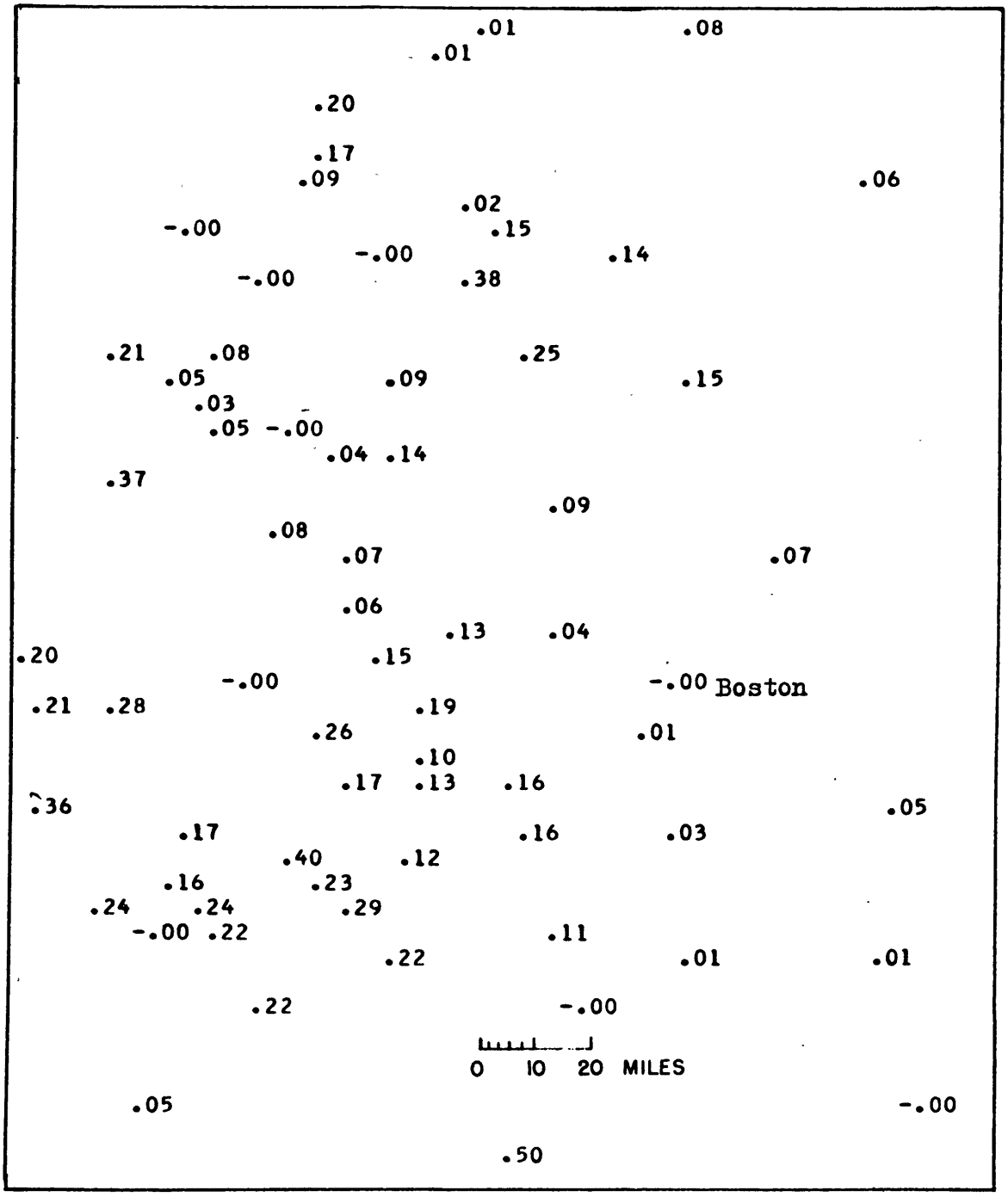

Figure 1. Example of computer-produced hourly precipitation map for 1500 EST, 12 December 1962. Location of Boston, Massachusetts and scale of miles have been added.

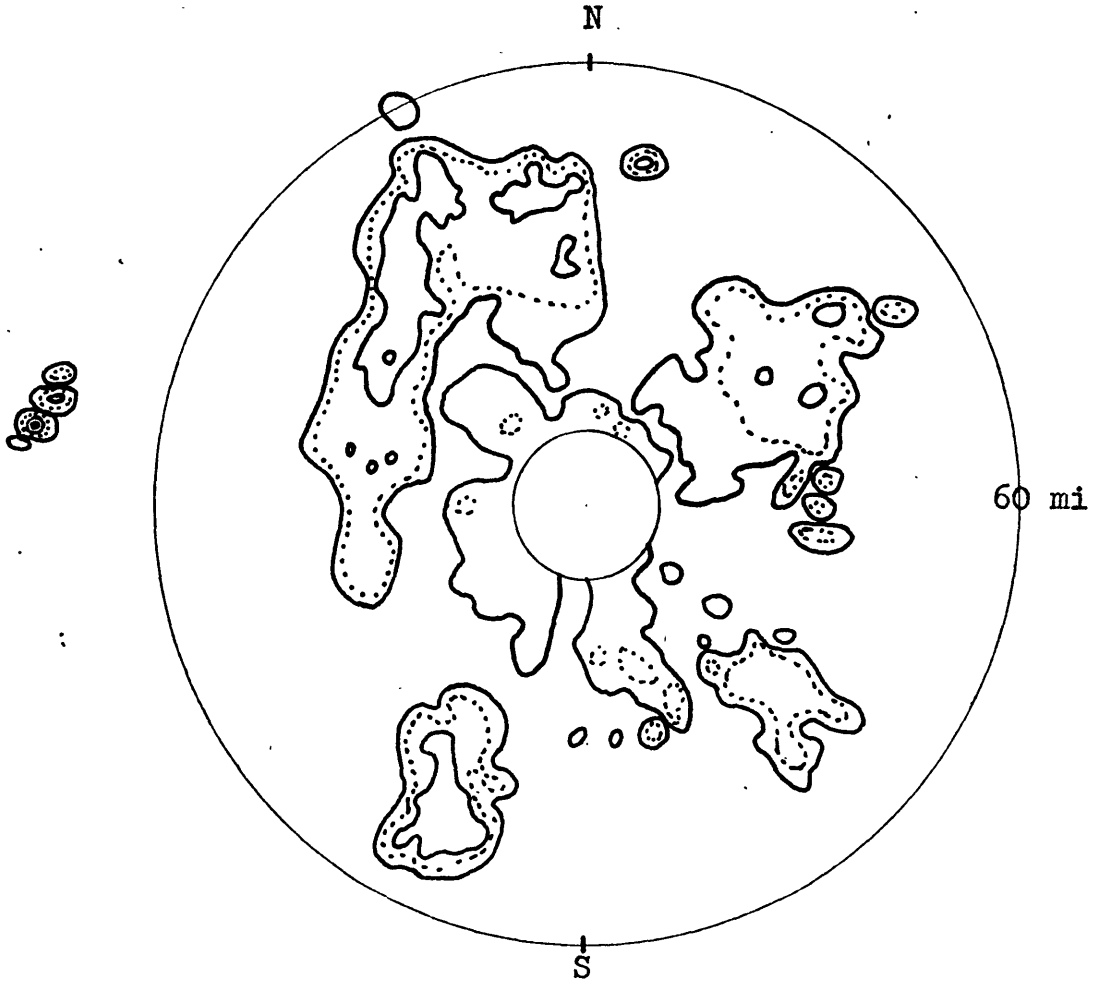

Figure 2. Example of map showing PPI sequence. Date: 18 May 1963. Time:: 1215 EST. Contours: 1, 2.5 (·····), 5, and 10 mm hr^{-1}.

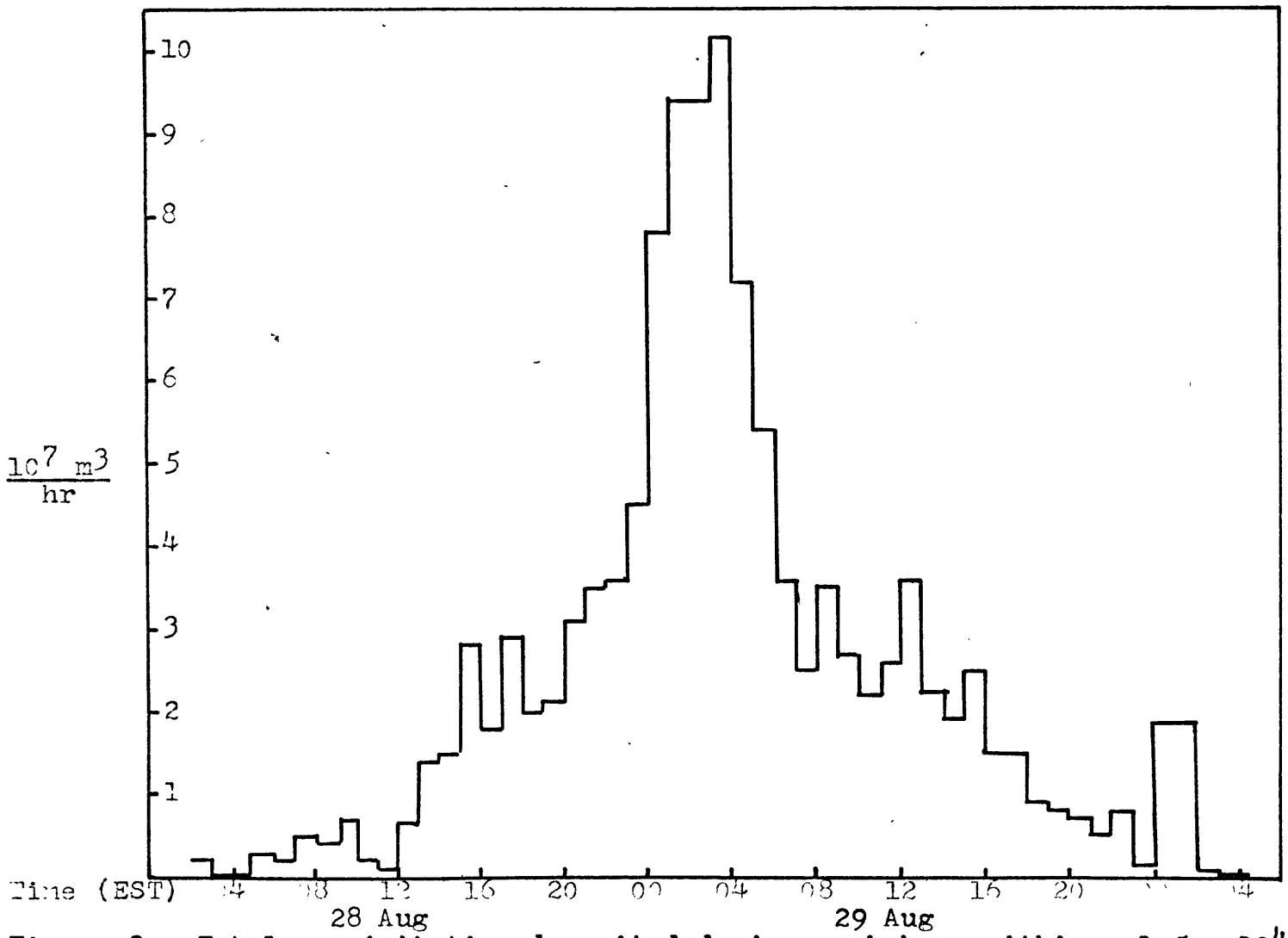

Figure 3. Total precipitation deposited during each hour within a 1.5×10^4 mi^2 area surrounding Cambridge, Massachusetts on 28-29 August 1962.

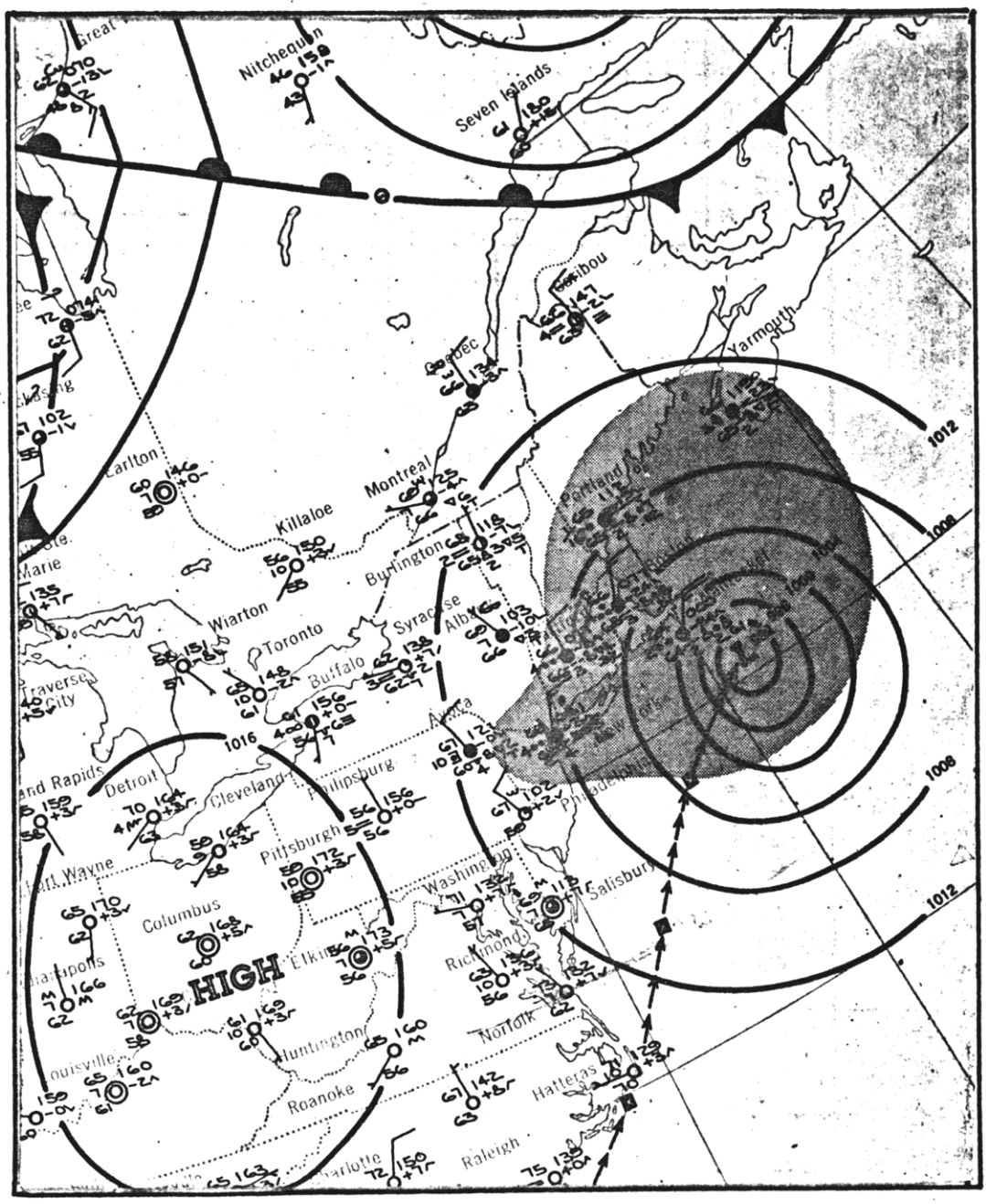

Figure 4. Surface synoptic map for 0100 EST, 29 August 1962.

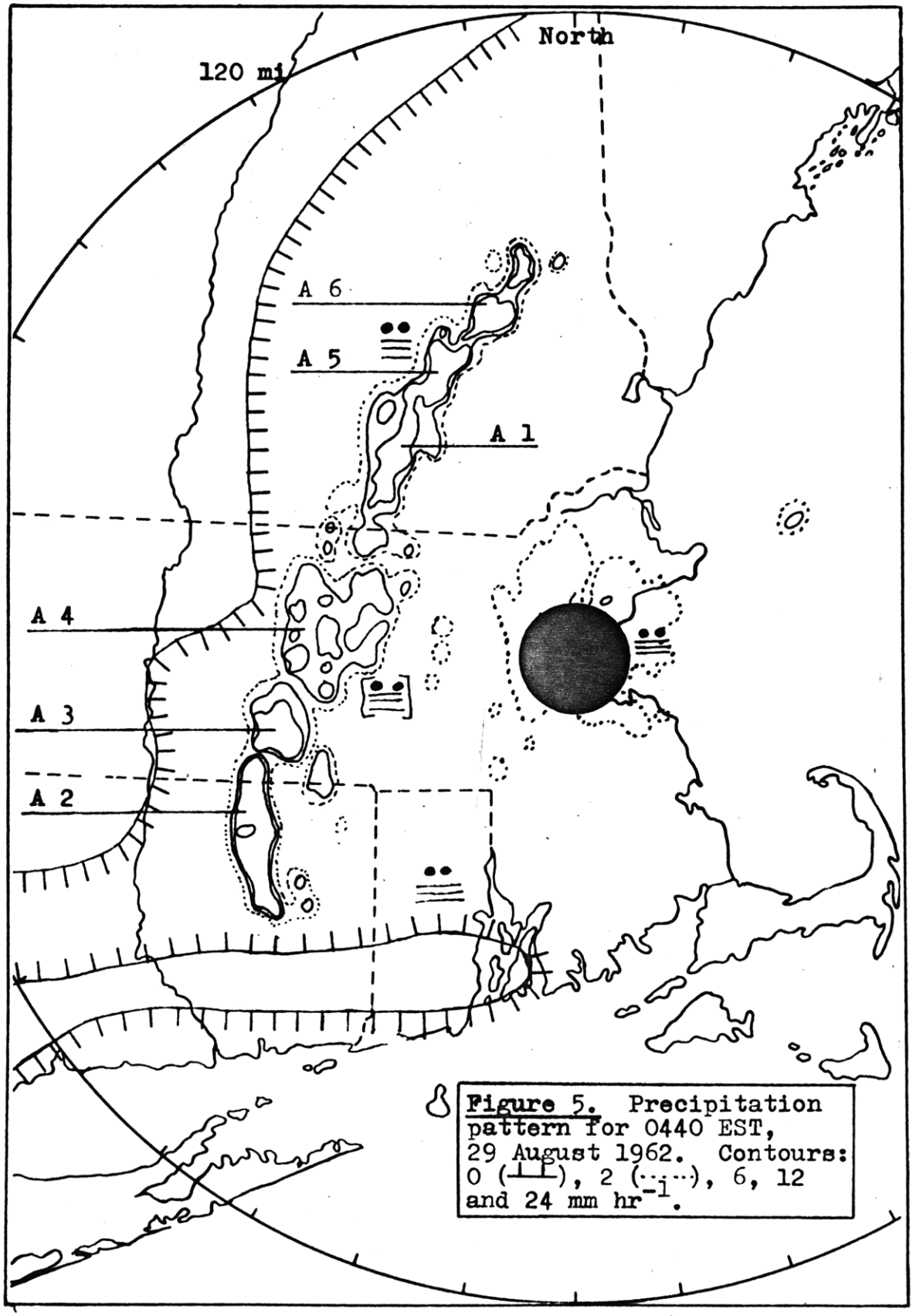

Figure 5. Precipitation pattern for 0440 EST, 29 August 1962. Contours: 0 (⊥⊥), 2 (··i··), 6, 12 and 24 mm hr^{-1}.

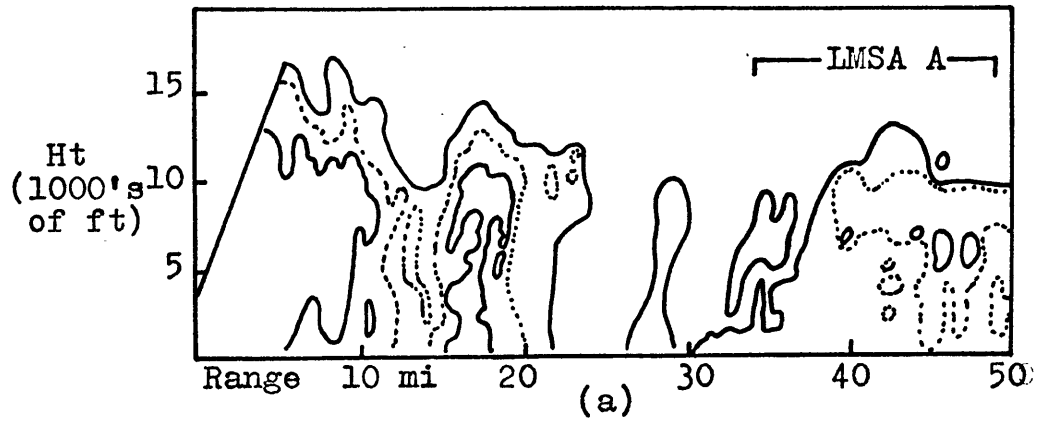

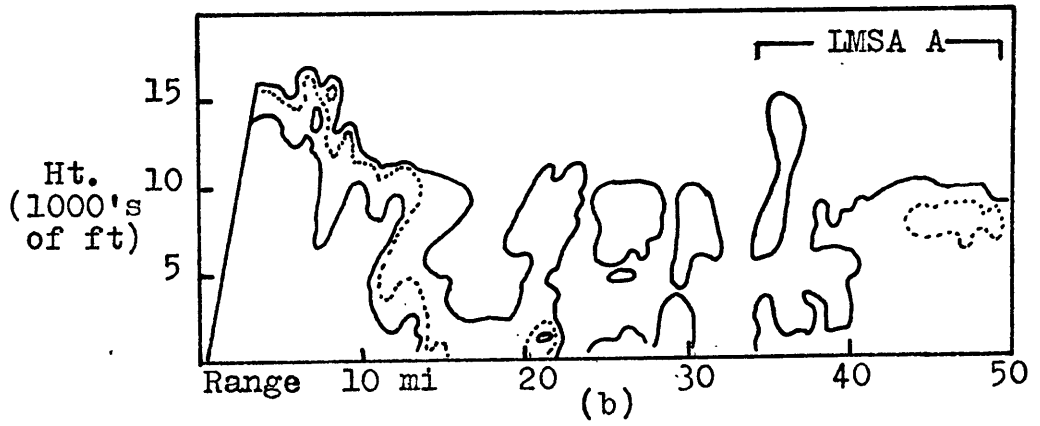

Figure 6. RHI patterns for 29 August 1962. Echoes at ranges 35-50 mi are from large mesoscale area A (LMSA A). (a) Time: 0420 EST. Azimuth: 290 degrees. Gain settings: 10, 8 (·····), 6. (b) Time: 0423 EST. Azimuth 320 degrees. Gain settings: 10, 8 (·····), 6.

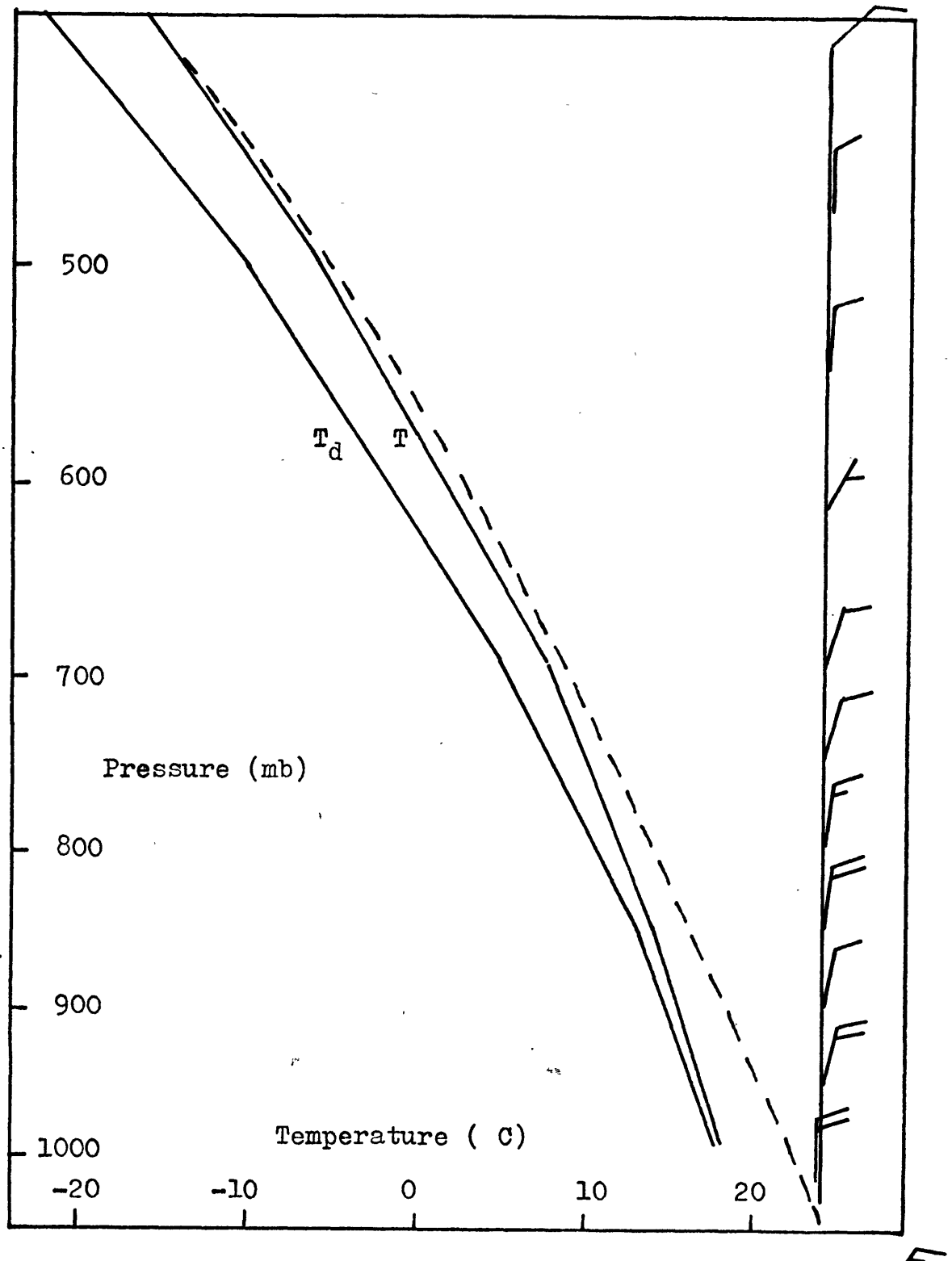

Figure 7. Temperature (T), dew point (T_d), and wind ( ) profiles for Nantucket, Massachusetts, 29 August 1962, 0700 EST. Dashed line is a pseudoadiabat.

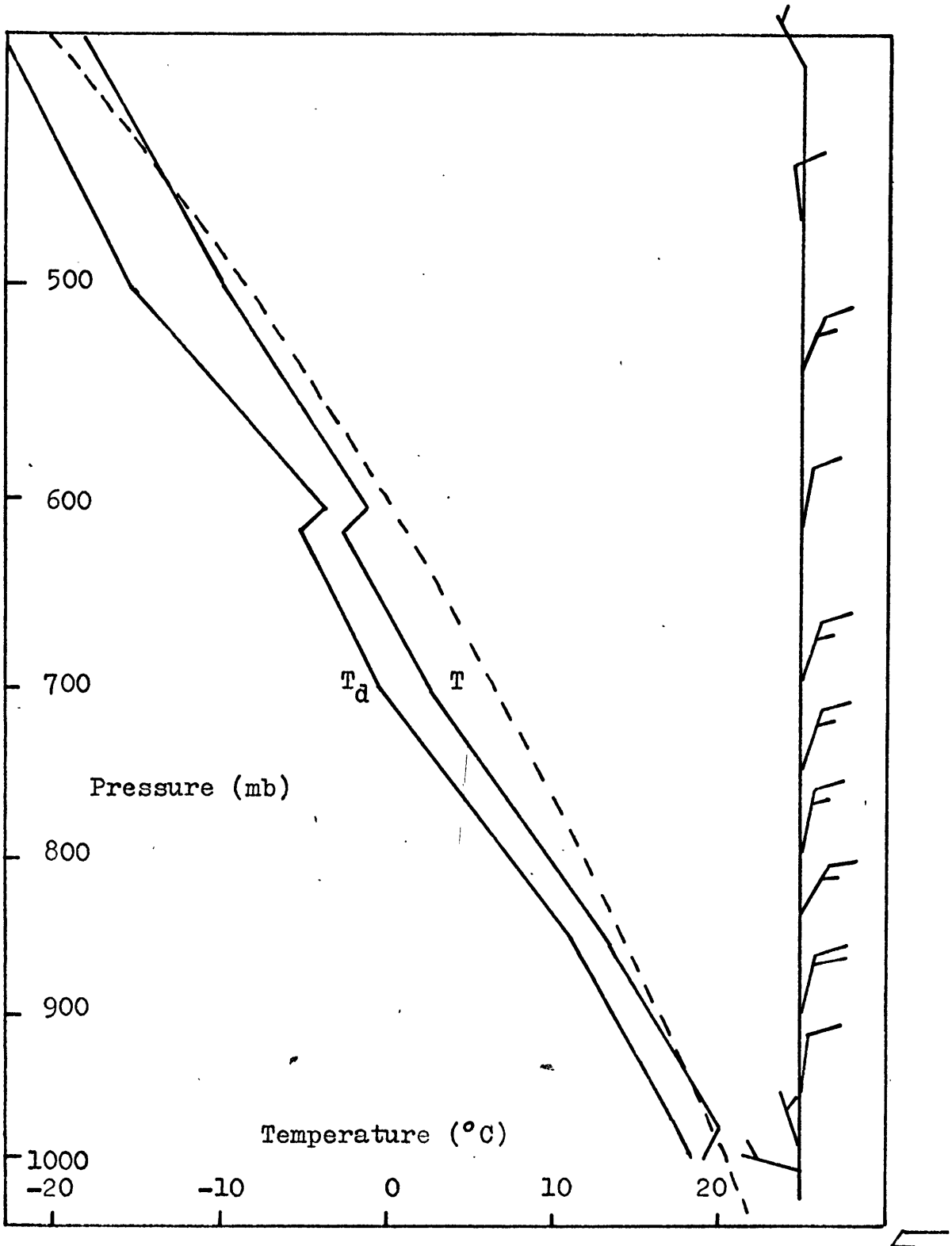

Figure 8. Temperature (T), dew point (T_d), and wind ( ) profiles for Albany, New York, 29 August 1962, 0700 EST. Dashed line is a pseudoadiabat.

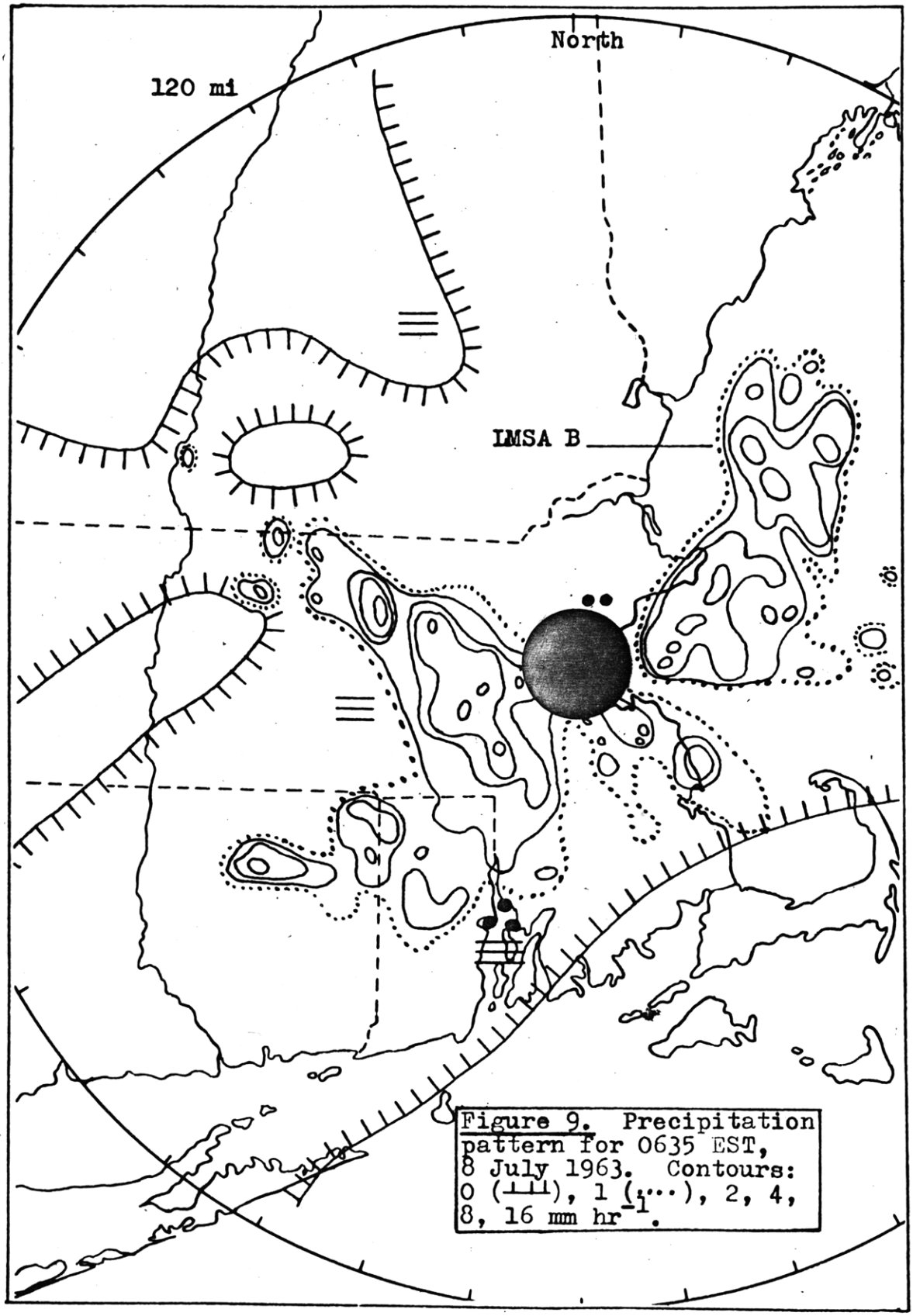

Figure 9. Precipitation pattern for 0635 EST, 8 July 1963. Contours: 0 (———), 1 (· · ·), 2, 4, 8, 16 mm hr^{-1}.

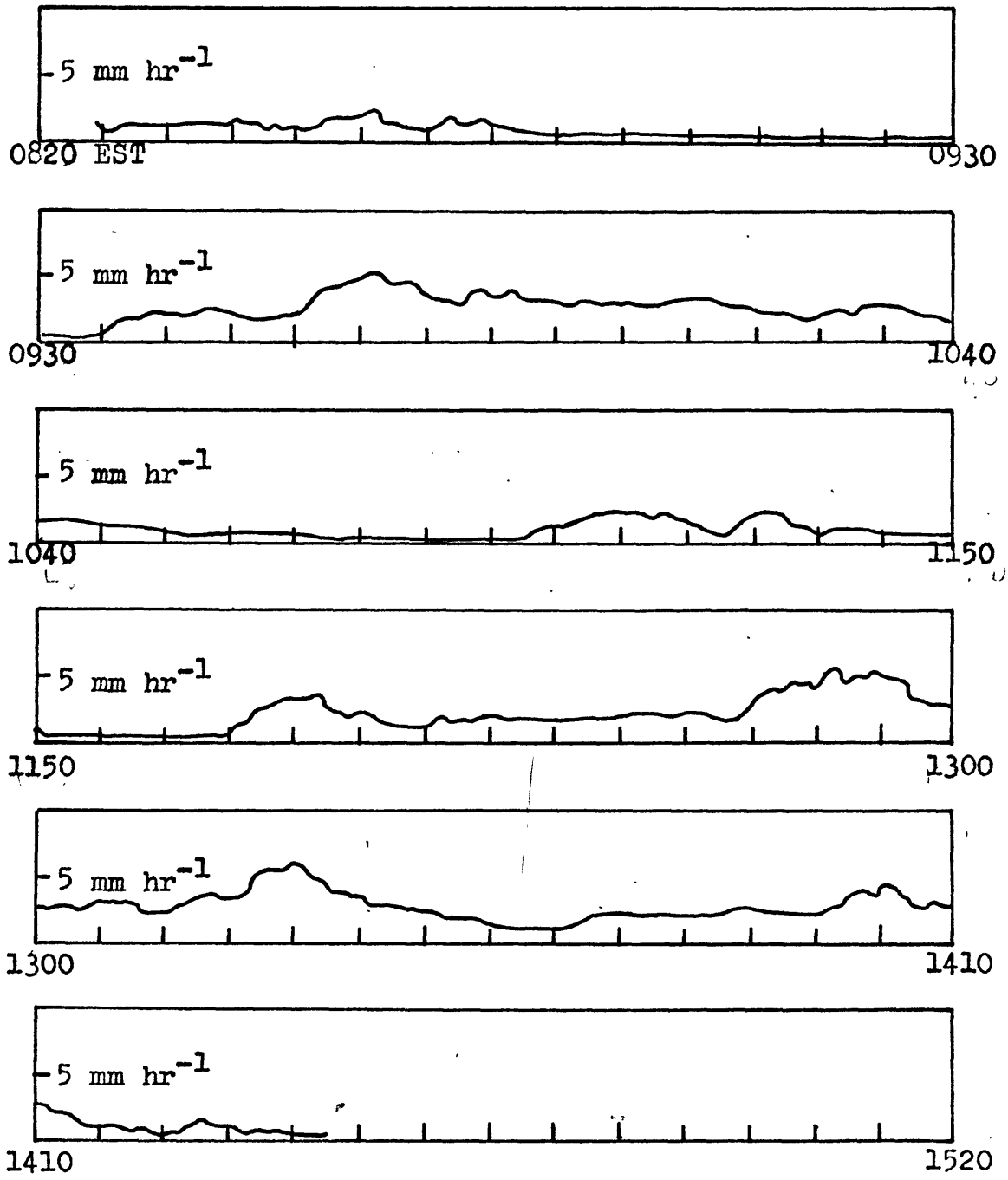

Figure 10. Detailed rain-gauge trace from West Concord, Massachusetts. 18 May 1963.

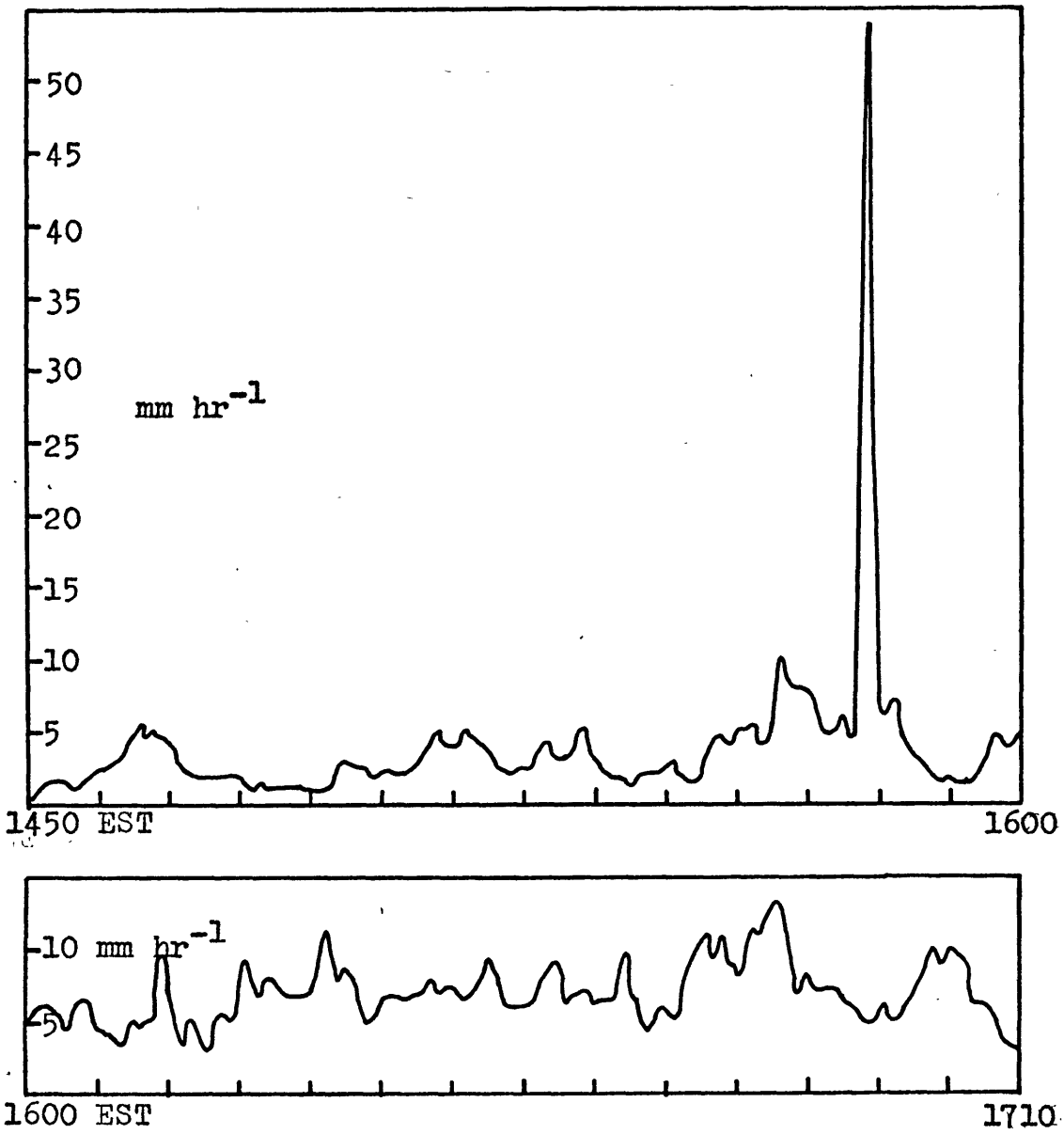

Figure 11. Detailed rain-gauge trace from West Concord, Massachusetts. 6 December 1962.

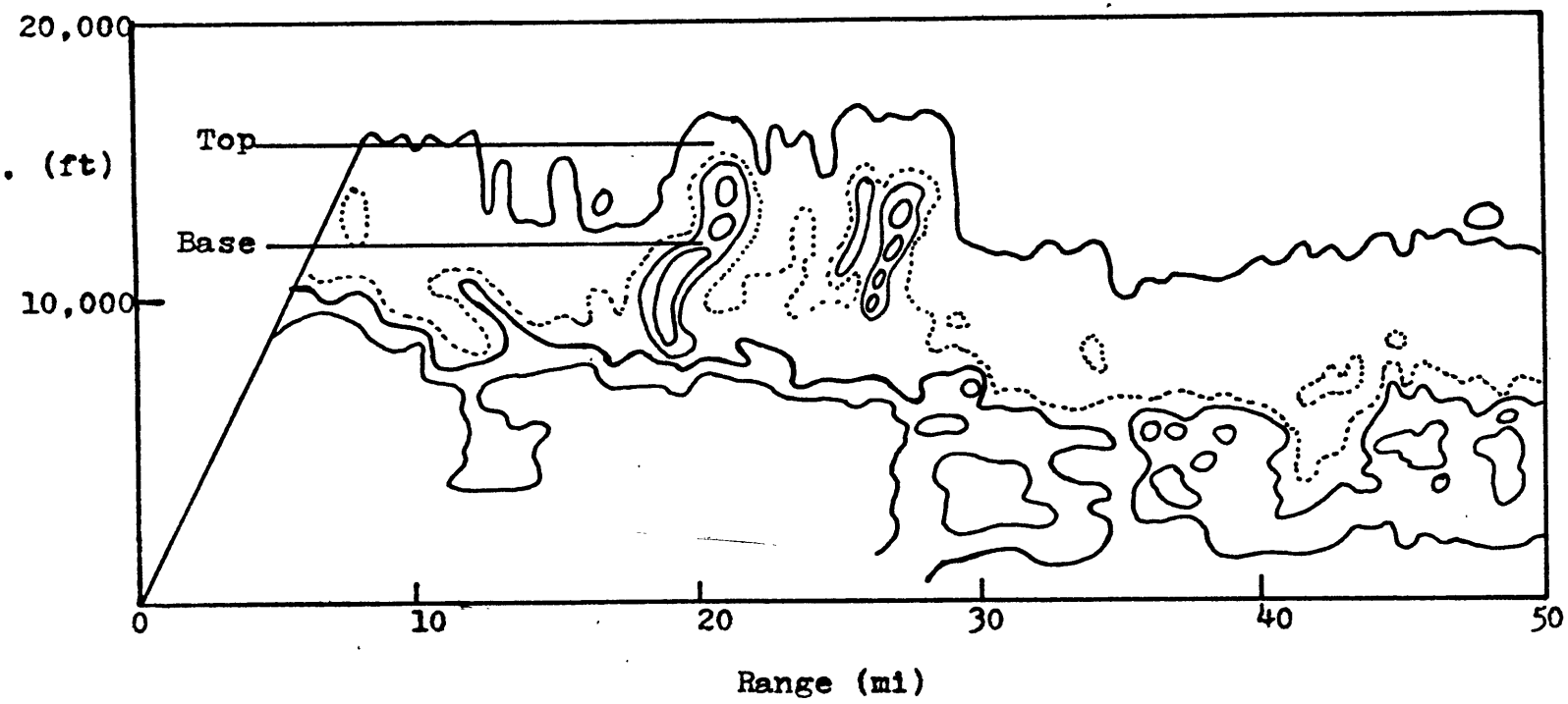

Figure 12. RHI pattern for 1443 EST, 12 January 1963. Azimuth: 348 degrees. Gain settings: 10, 8 (·····), 6,5.

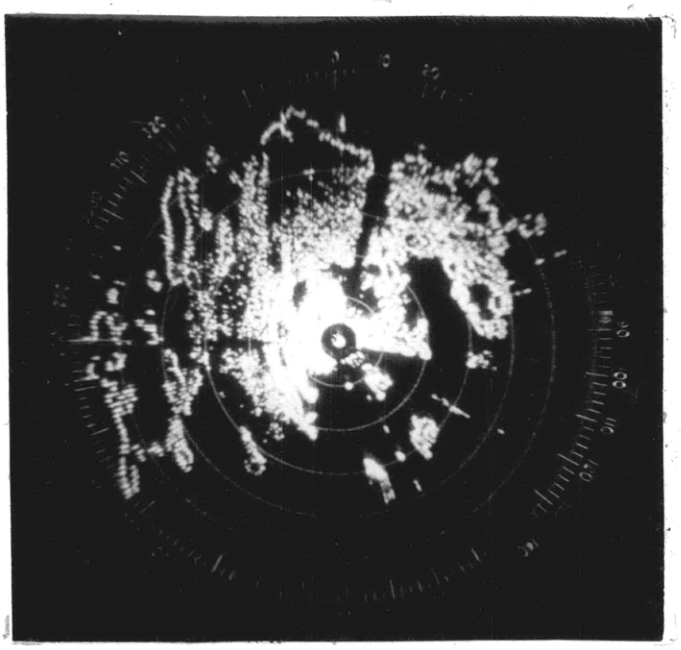

(a)

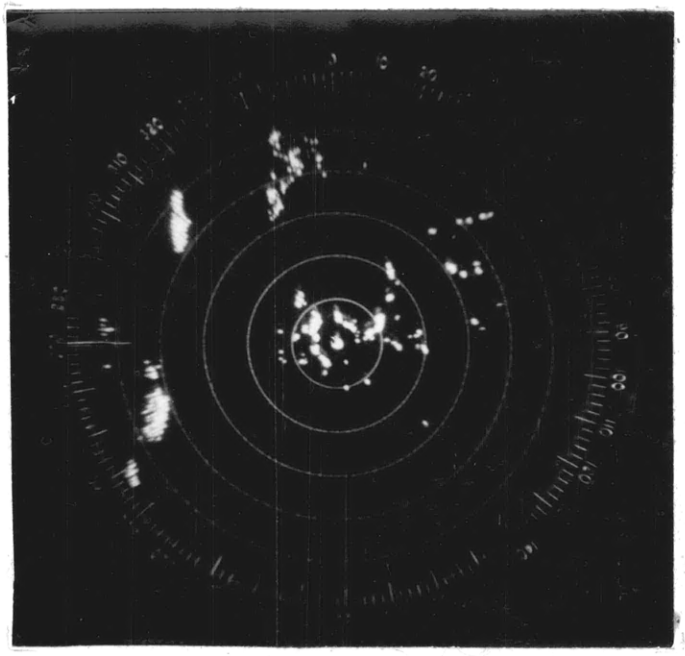

(b)

Figure 13. Typical PPI pattern on 2 February 1963. (a) Intensity level 2. (b) Intensity level 4.

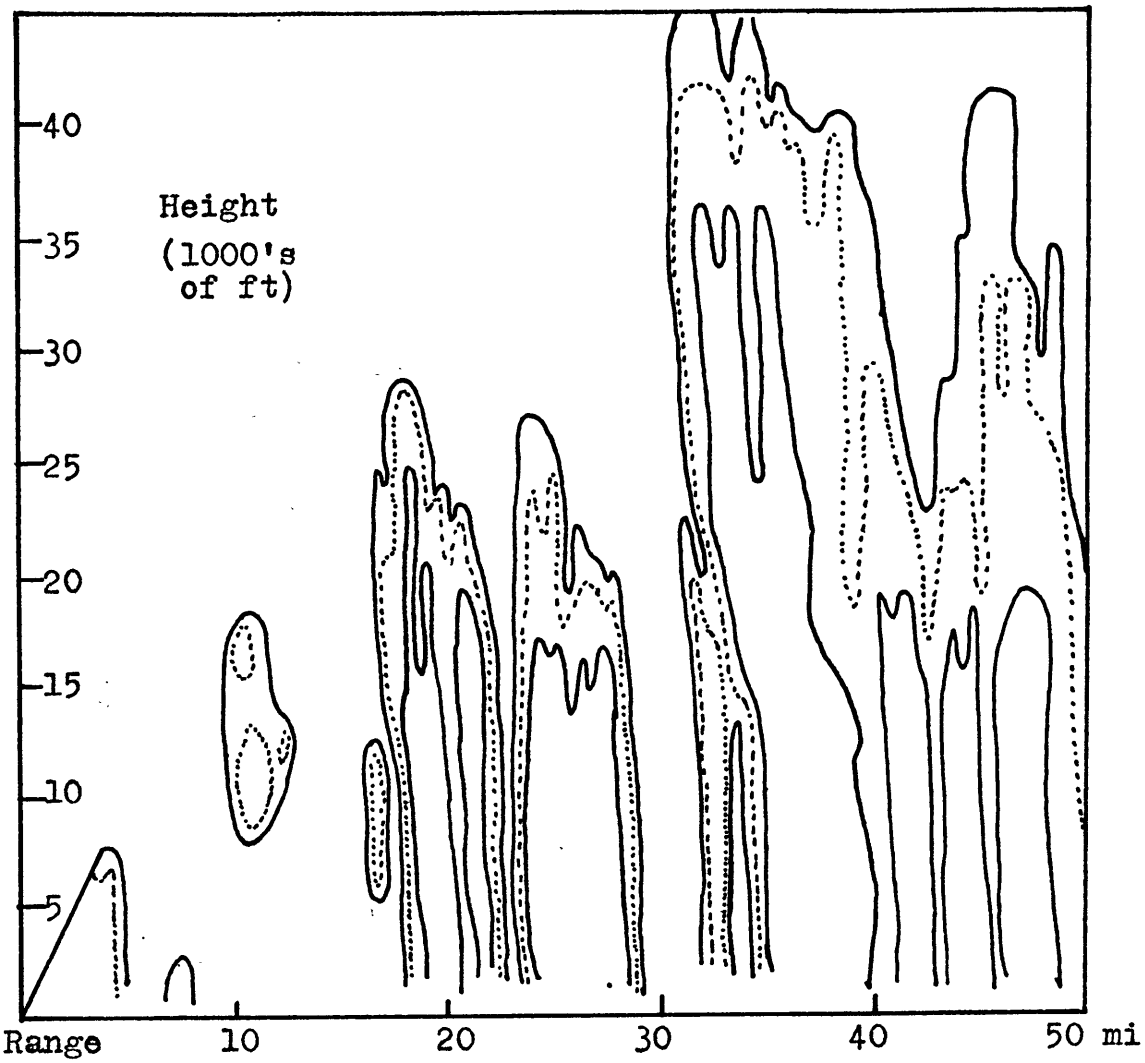

Figure 14. RHI pattern for 1538 EST, 8 July 1963. Azimuth: 350 degrees. Gain settings: 10, 9 (·····), 8.

Figure 15. Schematic representation of the precipitation patterns observed in each storm.

Legend:

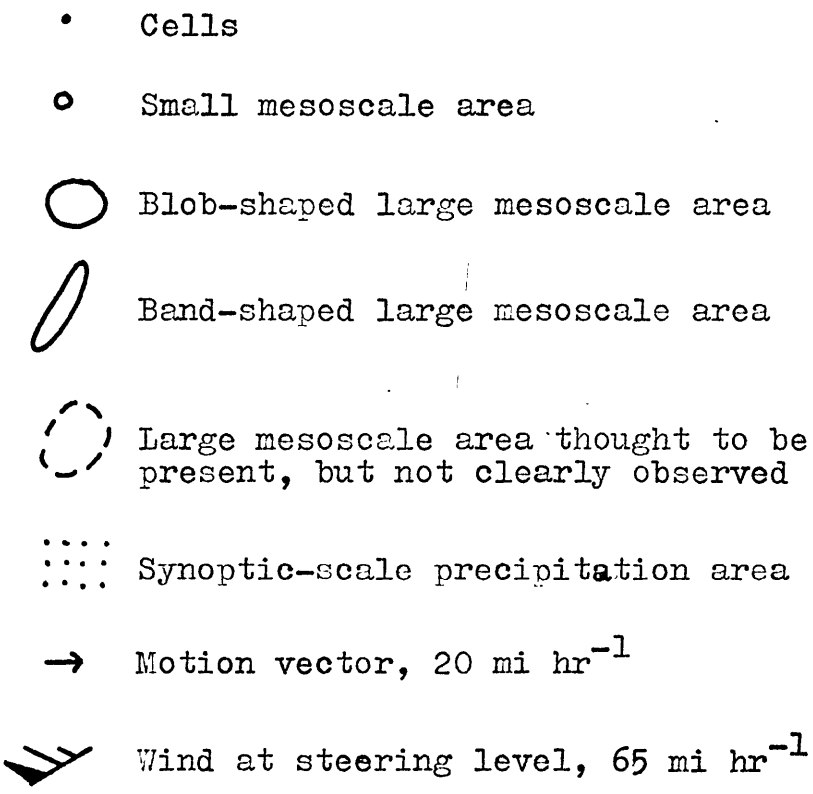

Fig. 15
(cont.)

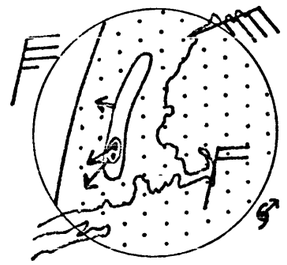

A. 29 AUG 62

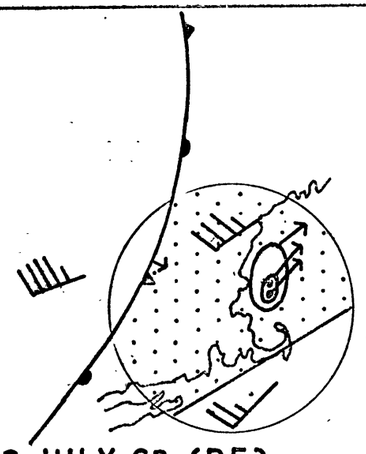

B. 8 JULY 63 (PF)

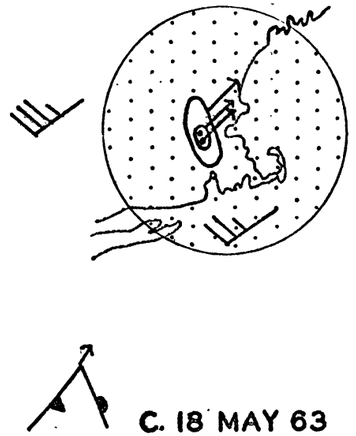

C. 18 MAY 63

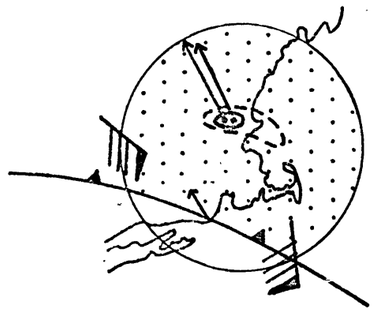

D. 6 DEC 62

E. 17 SEP 63

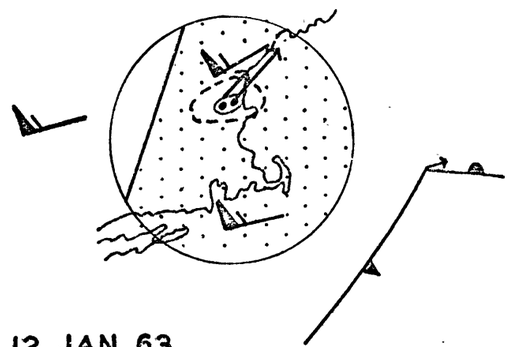

F. 12 JAN 63

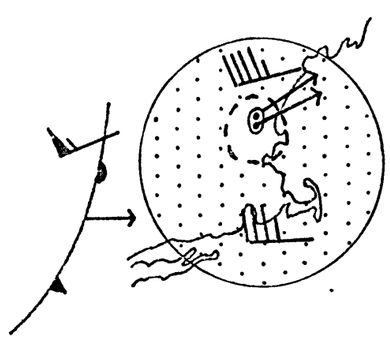

G. 2 FEB 63

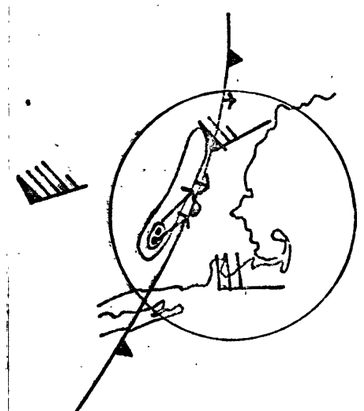

H. 8 JULY 63 (F)

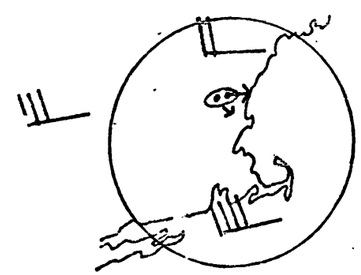

I. 9 JUNE 65

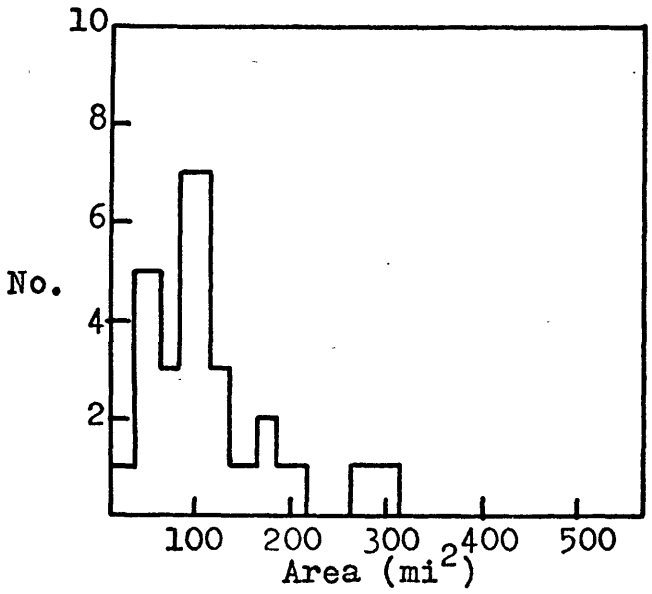

Figure 16. Histogram showing the number of small mesoscale areas (SMSA's) observed versus their average areas.

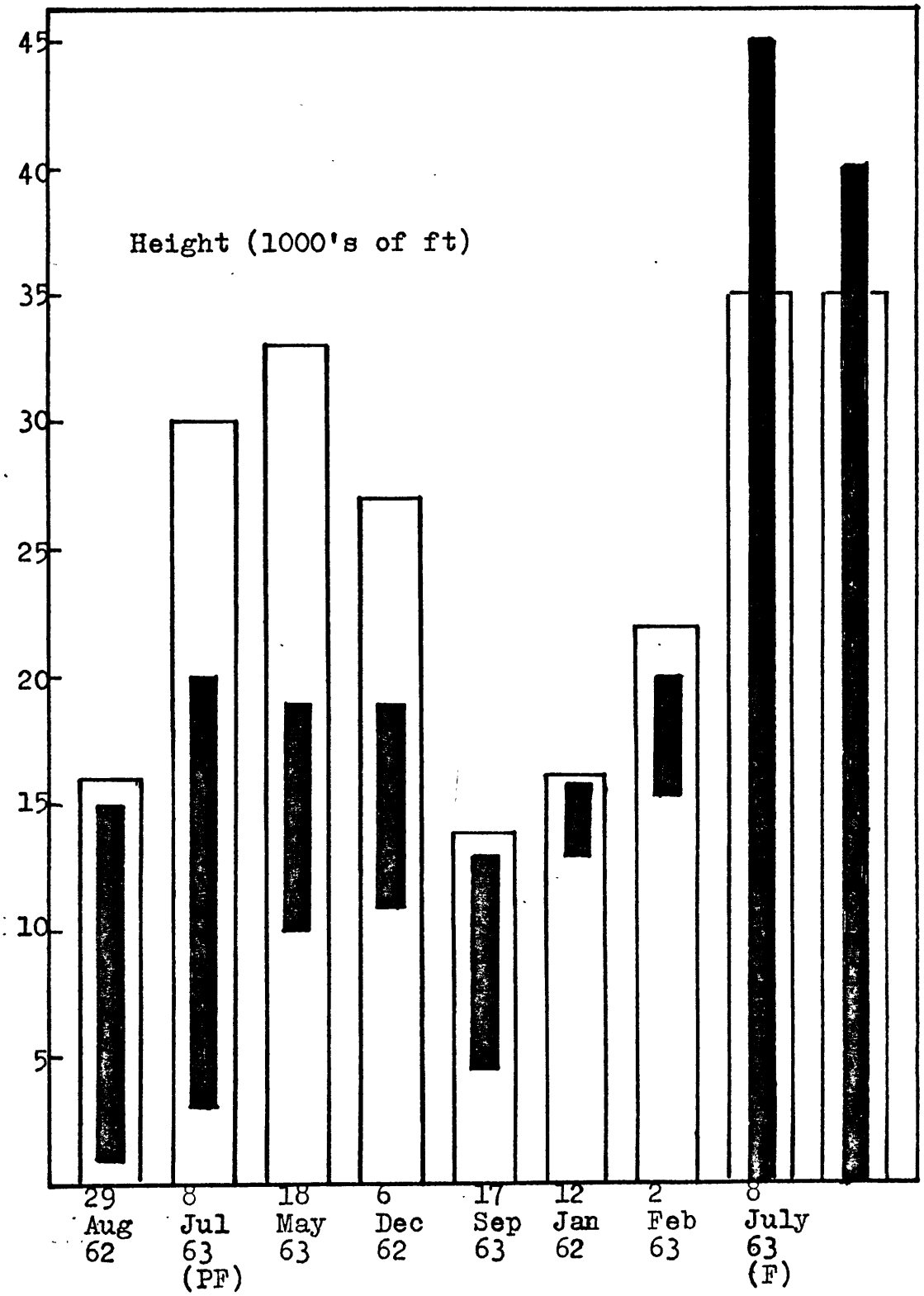

Figure 17. Diagram showing for each storm the layer containing the cells (shaded) and the layer of lighter precipitation surrounding the cells (unshaded).

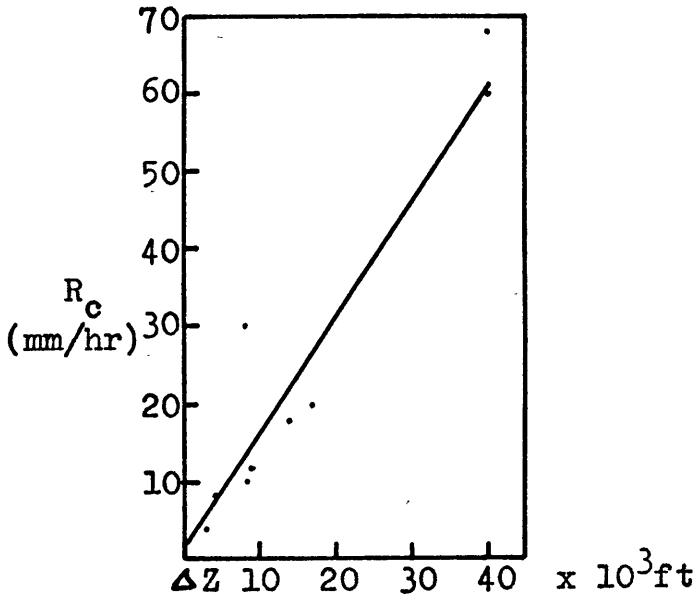

Figure 18. Cell intensity R_c versus cell depth ΔZ. Each point represents an average cell in a particular storm.

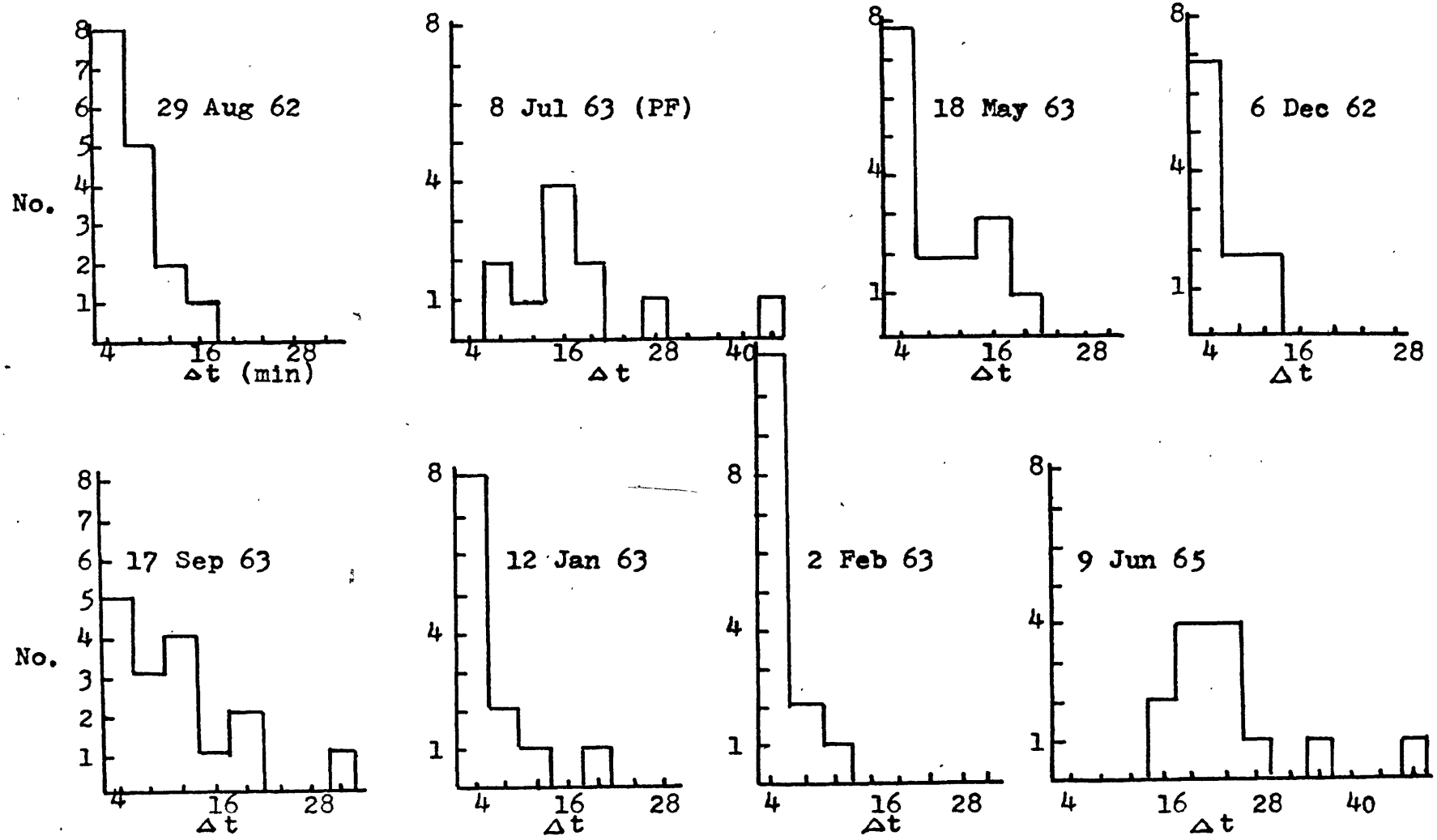

Figure 19. Number of cells observed versus their durations (Δt) for each storm.

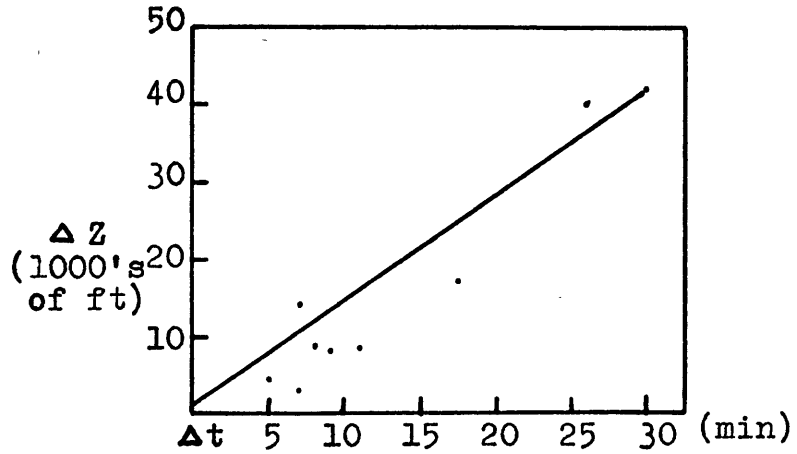

Figure 20. Cell depth (ΔZ) versus cell duration (Δt). Each point represents an average cell in a particular storm.

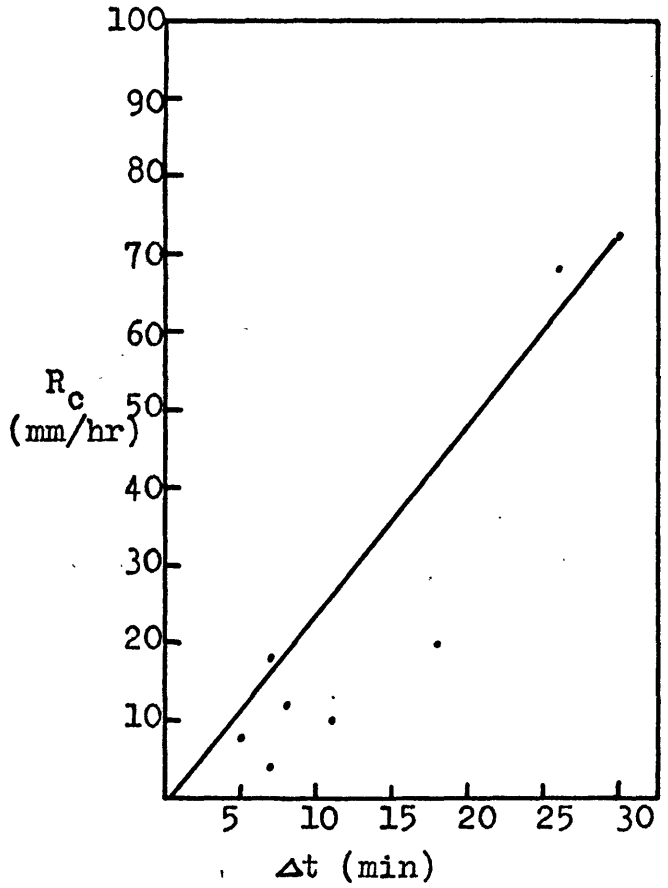

Figure 21. Cell intensity (R_c) versus cell duration (Δt). Each point represents an average cell in a particular storm.